

# Hierarchical Modeling and Architecture Optimization: Review and Unified Framework

Paul Saves<sup>1,a</sup>, Edward Hallé-Hannan<sup>b</sup>, Jasper Bussemaker<sup>c</sup>, Youssef Diouane<sup>b</sup>, Nathalie Bartoli<sup>d,e</sup>

<sup>a</sup>*IRIT and UT Capitole, Université de Toulouse, CNRS, Toulouse INP, UT3, UT2J, UT Capitole, Toulouse, France.  
paul.saves@irit.fr*

<sup>b</sup>*GERAD and Department of Mathematics and Industrial Engineering, Polytechnique Montréal, QC, Canada.  
{edward.halle-hannan, youssef.diouane}@polymtl.ca*

<sup>c</sup>*Institute of System Architectures in Aeronautics, German Aerospace Center (DLR), Hamburg, Germany.  
jasper.bussemaker@dlr.de*

<sup>d</sup>*DTIS, ONERA, Université de Toulouse, 31000, Toulouse, France.*

<sup>e</sup>*Fédération ENAC ISAE-SUPAERO ONERA, Université de Toulouse, 31000, Toulouse, France.  
nathalie.bartoli@onera.fr*

---

## Abstract

Simulation-based problems involving mixed-variable inputs frequently feature domains that are hierarchical, conditional, heterogeneous, or tree-structured. These characteristics pose challenges for data representation, modeling, and optimization. This paper reviews extensive literature on these structured input spaces and proposes a unified framework that generalizes existing approaches. In this framework, input variables may be continuous, integer, or categorical. A variable is described as *meta* if its value governs the presence of other *decreed variables*, enabling the modeling of conditional and hierarchical structures. We further introduce the concept of *partially-decreed variables*, whose activation depends on contextual conditions. To capture these inter-variable hierarchical relationships, we introduce *design space graphs*, combining principles from feature modeling and graph theory. This allows the definition of general hierarchical domains suitable for describing complex system architectures. The framework supports the use of surrogate models over such domains and integrates hierarchical kernels and distances for efficient modeling and optimization. The proposed methods are implemented in the open-source Surrogate Modeling Toolbox (SMT 2.0), and their capabilities are demonstrated through applications in Bayesian optimization for complex system design, including a case study in green aircraft architecture.

**Keywords:** Numerical modeling; feature model; hierarchical domain; meta variables; mixed variables; design space graph; Gaussian process.

---



---

<sup>1</sup>*First and corresponding author*

## Nomenclature

Abbreviation	Meaning
ADSG	Architecture Design Space Graph
BO	Bayesian Optimization
cat	Categorical variable
cont	Continuous variable
CR	Continuous Relaxation
DAG	Directed Acyclic Graph
dec	Decreed variable
DoE	Design of Experiments
DOT	DAG of tomorrow
DRAGON	Distributed fans Research Aircraft with electric Generators by ONERA
DSG	Design Space Graph
EI	Expected Improvement
EXC	Excluded
EMI	Earth Mover Intersection
FAST-OAD	Future Aircraft Sizing Tool with Overall Aircraft Design
FM	Feature Model
GED	Graph Edit Distance
GD	Gower Distance
HPO	Hyper-Parameters Optimization
GP	Gaussian Process
HH	Homoscedastic Hypersphere
int	Integer variable
KPLS	Kriging with Partial Least Squares
LCA	Lowest Common Ancestor
LHS	Latin Hypercube Sampling
met	Meta variable
MAP	Maximum <i>A Posteriori</i>
MLP	Multi-Layer Perceptron
MMD	Maximum Mean Discrepancy
NSGA2	Non-dominated Sorting Genetic Algorithm II
ord	Ordinal variable
PLS	Partial Least Squares
qtn	Quantitative variable
SBArchOpt	Surrogate-based Architecture Optimizer
SEGOMOE	Super Efficient Global Optimization with Mixture of Experts
SMT	Surrogate Modeling Toolbox
SPD	Symmetric Positive Definite
SVM	Singular Vector Machine
UCB	Upper Confidence Bound
WB2S	Watson and Barnes 2 <sup>nd</sup> -criterion Scaled

## 1. Introduction

Optimizing the architecture of complex systems, such as those related to aerospace design, requires the exploration of vast and highly intricate design spaces to identify optimal solutions [30, 40]. These design processes often depend on *expensive-to-evaluate* computer simulations, which are used to explore innovative concepts in early-stage studies and analyses [97]. Given input values, these computer models output key performance metrics, such as the aerodynamic efficiency of an aircraft, and because they are opaque, expensive, and derivative-free, they are considered as *blackbox* functions [9]. The design and optimization of such complex systems is further complicated by the large number of variables influencing their overall performance and feasibility. As system complexity grows, traditional methods for exploring design spaces become less practical due to the high computational cost and inherent complexity of the data structures involved [97, 142]. To address the inefficiencies of directly evaluating such simulations, the optimization process increasingly leverages *surrogate models*, which provide inexpensive approaches to evaluate the expensive objective or constraint functions. These surrogate models enable the efficient exploration of complex and high-dimensional design spaces, making them indispensable for the optimization of complex systems [97].

One of the critical challenges in this domain is the structured *heterogeneity* of the design spaces, characterized by diverse input data types and complex interdependencies. Real-world optimization problems typically involve a mix of continuous, integer, and categorical variables. In addition, some variables, called *decreed* may be included or excluded depending on the state of other variables known as *meta* variables, creating additional layers of hierarchy [72]. Consequently, such mixed-variable domains pose significant challenges that traditional optimization and modeling techniques often struggle to capture in a scalable and efficient manner, especially when the design space is structured and the relationships between variables are non-trivial [19]. Although the literature offers several approaches for tackling these challenges, ranging from Bayesian optimization and surrogate modeling to feature-based methods, no single solution has been consistently outperforming [149].

As a result, the field lacks a comprehensive framework that can unify these varied techniques and address the full spectrum of mixed-variable and hierarchical optimization problems encountered in complex system design. This paper also addresses a critical gap between the SMT library [23] and the Design Space Graph (DSG) software (adsg-core) [31], which is essential for fully integrating hierarchical surrogate modeling into the existing ecosystem. Our goal is to define distances and models for heterogeneous data points in mixed-variable domains, where two points do not necessarily share the same variables or bounds [72]. Such a domain is equipped with a single graph whose purpose is modelling the complex hierarchical dependencies. Although closely related, the proposed framework does not compare graphs, such as in graph matching. The framework focuses on the variables that can be present across the different data configurations. However, note that graph distances are covered in the literature review, since some notions of these are integrated in the framework and they share similar purposes.

This work is motivated by various real-world applications where meta variables play a pivotal role. For example, thermal insulation design involves meta variables that dictate the number of heat intercepts, each introducing new design variables [2, 86]. Similarly,

in aerospace design, meta variables influence critical decisions such as the number of engine shafts or the inclusion of a fan [34, 15, 32]. The general context of this research lies in system architecture, which defines how systems meet stakeholder requirements by specifying components, functions, and their interrelationships [48]. Designing system architectures involves complex decision-making, requiring cross-disciplinary collaboration and effective management of requirements and functions [40, 128]. Our approach is validated through a case study on green aircraft design optimization using Bayesian Optimization (BO) techniques, demonstrating the framework’s ability to manage hierarchical dependencies and complex variable structures. This paper builds upon prior work connecting hierarchical variable frameworks with surrogate-based modeling and optimization [72, 131, 32], aiming to integrate these frameworks within more general system architecture environments [30, 31, 41].

This paper provides a comprehensive review of multiple research domains, identifying critical intersections and synergies in the existing literature. Then, this paper proposes a unified framework for surrogate modeling in architecture optimization, building on these findings. Leveraging *graph theory* concepts, its goal is to extend existing concepts through a generalized approach capable of handling mixed-variable and hierarchical blackbox functions and simulations. To finish, this paper delivers the first open-source implementation of the developed framework, enabling the resolution of diverse heterogeneous modeling problems in practical applications. Our main contributions are:

1. Conduct an extensive review of graph kernels and hierarchical variable models to contextualize their applications and to showcase their applicability in managing hierarchical dependencies and complex variable structures particularly for defining distances or correlation kernels.
2. Propose a unified mathematical framework enabling for more expressive and flexible modeling of dependencies. This generalization provides a robust foundation for addressing hierarchical and conditional variable relationships. A distance is proposed to compare two hierarchical input points and build a correlation kernel for surrogate modeling.
3. Implement this framework in the open-source SMT toolbox [135], extending its capabilities to support hierarchical surrogate models. This implementation is documented in a dedicated tutorial notebook<sup>2</sup>, easing its practical application.

The remainder of this document is structured as follows. Section 2 reviews related work, focusing on surrogate modeling in variable-size spaces, representations of structured data, and general distance measures over such structures. Section 3 introduces our extended framework, detailing the hierarchical distance and kernel, the automation of the underlying graph construction, and demonstrating its use through a case study on multi-layer perceptron architectures. Section 4 applies the framework to surrogate modeling for Bayesian optimization, concluding with a real-world application to green aircraft optimization. Finally, Section 5 summarizes our contributions and outlines directions for future research.

---

<sup>2</sup>[https://github.com/SMTorg/smt-design-space-ext/blob/main/tutorial/SMT\\_DesignSpace\\_example.ipynb](https://github.com/SMTorg/smt-design-space-ext/blob/main/tutorial/SMT_DesignSpace_example.ipynb)

## 2. Literature review

This section provides a literature review of related works and previous studies. Specifically, it reviews key approaches to handling variable-size spaces, data representations, and distance measures over complex structures.

### 2.1. Background and previous works

This section describes meta and meta-decreed variables, which model hierarchical dependencies in domains of interest, as introduced in previous works [8, 71] and [72], respectively. This framework has been formally analyzed through a so-called design space graph introduced for an application to hybrid-electric distributed propulsion aircraft [133] and compared with the classical Feature Model (FM) [17].

#### 2.1.1. Types and roles of variables

For a given problem featuring  $n$  variables, a point  $\mathbf{X}$  can be decomposed as  $\mathbf{X} = (X_1, \dots, X_n)$ , where  $X_i$  is the value taken by the point  $\mathbf{X}$  in its corresponding  $i^{\text{th}}$  variable. To incorporate structure into the problem, it is necessary to establish a terminology that describes the types and roles of variables. Each variable is assigned a *type* that reflects its quantitative or qualitative nature [132, 32], four types that can be assigned to a variable:

- continuous, if the variable can take any real value between lower and upper bounds;
- integer, if the variable can take any integer value between lower and upper bounds;
- ordinal, if the variable can take any value in a ordered finite set of either strings or values;
- categorical, if the variable can take any value in an unordered finite set of either strings modalities or values.

In addition to their variable type, each variable is assigned a *role* that reflects its hierarchy with other variables in points of the hierarchical domain [8, 72]. An underlying graph structure models the hierarchy between variables through parent-child relations. In this graph, a variable  $x_i$  is a parent of another variable  $x_j$  (a child), if  $x_i$  controls the inclusion or bounds of  $x_j$ , with  $i, j \in \{1, 2, \dots, n\}$ . In such cases,  $x_j$  is said to have a *decree dependency* with  $x_i$ , and an arc from  $x_i$  to  $x_j$  is present in the graph. This arc represents the decree dependency. More details on the graph structure are provided in the next section. The roles of the variables, *variable roles* for short, are determined based on whether they have parents and/or children in the graph. Each variable is assigned one of the following four roles:

- (strictly) meta, if has no parent and at least one child;
- meta-decreed, if has at least one parent and at least one child;
- (strictly) decreed, if it has at least one parent and no children;
- neutral, it neither has parent or children.

### 2.1.2. Modeling Design Spaces featuring Graph Structures

This section presents references addressing the general class of problems that involve hierarchical spaces in the context of data-driven regression and optimization. In this study, a hierarchical space, originally introduced in [76], is defined as a space with at least one meta variable, following the formalization in [72]. A hierarchical space may also be referred to as a variable-size space [113], as a conditional search space problem [13], as an heterogeneous dataset [122] or as a hierarchical domain [72]. More details about other data structure representations are given in [Appendix A](#).

Decreed and meta-decreed variables may have multiple parents, and both types can influence numerous other variables. Building on these observations, we introduce the role graph—a structure that captures all information about variable roles and decree dependencies. Formally, the role graph  $G = (N, A)$  is a couple, where  $N$  is the set of all the variables represented as nodes of the problems and  $A$  is the set of decree dependencies represented as arcs. In [72], a general class of mixed-variable hierarchical structures within domains was introduced. This work rigorously defines a hierarchical domain, denoted as  $\mathcal{X}_G$  that represents a domain  $\mathcal{X}$  equipped with a graph structure  $G$ . In this domain, each point  $\mathbf{X}$  is properly defined within  $\mathcal{X}$ , and the variables are hierarchically ordered in  $G$ , where a variable is a child of another if it is decreed by it. Equivalently, the domain is *hierarchical* if its corresponding role graph contains at least one decreed variable (i.e., a variable with the decree property). Additionally, the hierarchical domain framework introduced in [72] models mixed-variable domains with meta variables, implying that points do not necessarily share the variables or bounds. This hierarchical domain  $\mathcal{X}_G$  can be extended to contain the variables that may be considered excluded, i.e., variables decreed excluded due to the corresponding meta variable values in a given point. This extension yields a space, called the *extended domain*, containing all the possible variables that are present in at least one point. The role graph contains the decree dependencies and allows to condition universal sets into restricted sets. It is assumed to be directed and acyclic to avoid pathological situations where meta-decreed variables influence each other. Nevertheless, the Design Space Graph (DSG) addresses this issue by parsing the design variables through a recursive process, stepping through the included (but not-yet-parsed) choices. Typically, parsers process design variables in a sequential, left-to-right manner. However, due to the complex interdependencies among design choices in systems like Architecture Design Space Graph (ADSG), a simple sequential parsing approach may not suffice. To address this, the DSG employs a recursive parsing strategy. This method allows the parser to navigate through the network of design variables, processing each based on its dependencies rather than its position in a sequence. This recursive approach ensures that all design variables, including those not initially parsed due to their position or dependencies, are eventually analyzed, leading to a more comprehensive understanding of the system’s design structure [31].

The “**DRAGON**” aircraft concept [137] relies on a distributed electric propulsion aircraft, improving fuel efficiency by optimizing propulsive performance. **DRAGON** introduces multiple compact electric fans on the wing pressure side, increasing the bypass ratio as an alternative to large turbofans. This design overcomes challenges of under-wing turbofans while enabling transonic flight. In such aircraft design examples, a meta-decreed variable could be the number of motors that is used for a given wing, where each motor has a set of decreed

variable. Figure 1 illustrates the roles of variables for a toy example of a wing aircraft design with meta-decreed variables. The number of motors per wing  $m$  is a meta variable, since it controls how many variables, peculiar to each motor are in the problems ( $m = 0$  means single-engined aircraft as the engine is not supported by the wing). The number of propellers  $p_i$  assigned to the  $i$ -th motor is a meta-decreed variable since 1) its inclusion depends on the number of motors  $m$ , *i.e.*, it is decreed, and 2) it controls the amount of variables regarding the radii of every included propeller. Finally, the radius  $r_{ij}$  of  $j$ -th propeller in the  $i$ -th motor is a decreed variable, since its inclusion depends on the number of propellers  $p_i$  for the motor  $i$ .

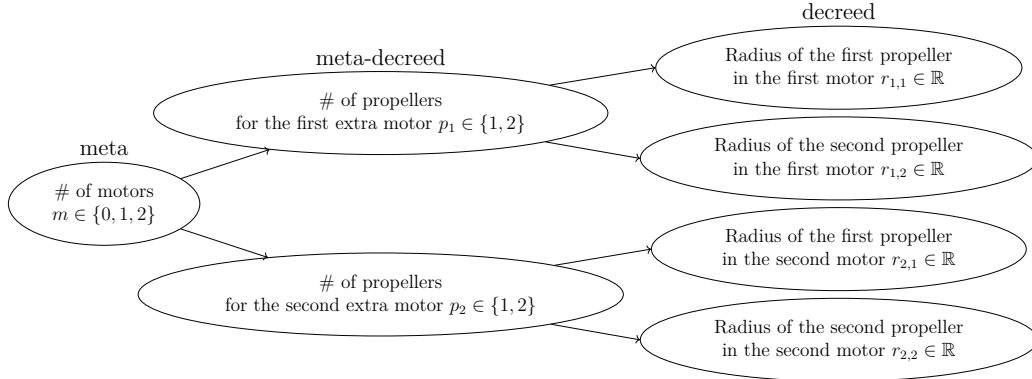


Figure 1: Variables roles for aircraft design problem.

In Figure 1, to compute the meta distance, we consider the extended points that contain all included and excluded variables. The variables that are excluded for a given point are assigned the special value **EXC**. In other words, some variables may be excluded for a point  $\mathbf{X} \in \mathcal{X}$  but present in another point  $\mathbf{X}'$ . For example, in Figure 1, the variable representing the number of propellers of the second motor is set to  $m_2 = \text{EXC}$ , when the number  $m$  of motors is one. Considering excluded variables provide necessary information for computing distances between points that do not share the same variables. This trick is always possible by adding bounds for every variable: for example, if we only have data for an aircraft with 2 motors and 2 propellers, we can always restrict the extended design space without loss of generality. Consequently, the extended domain, in which extended points reside, is constructed directly with Cartesian products on the bounded restricted sets of each variable. The hierarchical distance is defined on the extended domain but fortunately, a bijection based on the role graph  $G$  enables the mapping of points to extended points by adding **EXC** to the excluded variables, and conversely, maps extended points back to original points by removing variables assigned the value **EXC**. Thus, a distance function, that considers all included and excluded variables, is also induced on the original domain within the restricted set. For example, one of such distance combines angular and length information, and is well-defined for heterogeneous data comparison [72]. As such, it has the property of leading to unit induced distances when comparing a variable's well-defined value with a non-included variable whose value is **EXC**. This unit distance is effective for multiplication-based comparisons as it will be non-influential if multiplying the remaining distances by 1.



### 2.1.3. Hierarchical spaces with feature models

To describe complex configuration spaces—where selecting a high-level option determines the availability of related sub-options—we rely on *feature models*, a formalism widely used in software engineering [26]. In this context, a *feature* represents a configurable aspect of a system, such as a module, parameter, or capability that can be enabled or disabled. This directly corresponds to the notion of variables in hierarchical modeling, where the activation of one variable governs the inclusion or structure of others [17]. For example, in aircraft design, the feature “Energy source” might offer alternatives such as “Electricity” or “Fuel”, each unlocking its own specific set of design parameters. In this sense, features may correspond to variable levels, variables themselves, or even the domains (supports) of those variables. While feature models often define these roles loosely, we adopt a more structured interpretation in this work by treating features as the *nodes* of a DSG, a formalism we build upon in subsequent sections [7, 31]. In a feature model, features are organized via a tree structure, where nodes represent features and edges define dependencies. A child feature is only accessible if its parent is selected. Some are *mandatory*—always included when the parent is included—while others are *optional*. Groups of child features can also form exclusive (XOR) or inclusive (OR) sets, expressing constraints like “select exactly one” or “select at least one.” In addition to the tree, *cross-tree constraints* allow logical rules between features in different branches. These include relations such as “A requires B” or “A excludes B”, as well as more complex logical relationships as in “A and B implies not C” [16]. Feature models provide a compact way to describe rich, structured design spaces without enumerating every valid configuration. In our setting, they naturally map to hierarchical variable spaces, where high-level meta-choices conditionally activate relevant subsets of parameters.

## 2.2. Hierarchical surrogate modeling

This section first reviews surrogate-modeling strategies for representing architectural decision variables. It then tackles the core challenge of defining valid distance metrics in these complex, non-standard design spaces.

### 2.2.1. Hierarchical design spaces for surrogate modeling

Interest in modeling “variable-size” spaces emerged from various disciplines around 2010. For example, the work by [74] introduced Latin Hypercube Sampling (LHS) and Gaussian process (or Kriging) for *nested* variables, where variables depend hierarchically on other variables. Although the mechanisms differ, these nested variables can be considered akin to decreed variables in this context. Similarly, the technical report [76] from 2013 proposes a mixed-variable kernel function for varying-size spaces, referred as hierarchical. The latter report has been a key reference for the previous work [72], thus, it is also important for this current work. In this report [76], the inclusion and exclusion of a variable is controlled by variable-wise Kronecker delta functions. More precisely, the domain is equipped with a Directed Acyclic Graph (DAG) structure that contains hierarchical dependencies between the variables and where the variables are viewed as nodes. The inclusion of a (child) variable is determined by a delta function that takes the values of its ancestors, that is, variables of higher hierarchy that share a path in the DAG. The root and intermediate nodes are restricted to categorical variables. The kernel is constructed variable-wise with multiplication and addition of one-dimensional kernel. Each one-dimensional kernel is computed with



an assigned isometry, which is a distance-preserving function that maps a variable into a Euclidean space [56]. The computation of a one-dimensional kernel is divided into three cases: the variable is included for both points or the variable is excluded for both points or the variable is included for one and only one point.

In a Bayesian optimization context, the paper [114] proposes kernel functions that allow the construction of GP on domains with dimensional variables [93, 94], which are a special case of strictly discrete meta variables that influence the dimension and propose two kernels. First the subproblem-wise kernel computes similarity measures between dimensional variables, as well as between the other included variables, whose inclusion can be determined by dimensional variables. Second, the dimensional variable-wise kernel decomposes the computation dimensional variable per dimensional variable, which allows to regroup the specific decreed variables that are included by their corresponding dimensional variables [74]. For SVM regression, the work [63] proposes the Earth Mover’s Intersection (EMI or discrete Wasserstein) that computes similarity measures between sets of different sizes, similarly as the Jaccard index [150]. A kernel function is induced from the EMI, and SVM regression experiments are realized.

Going back to GP regression for hierarchical design spaces, defining valid and efficient covariance kernels over unordered sets of vectors presents unique challenges. Traditional kernels, like the squared exponential kernel, often fall short when applied to sets with no inherent ordering and varying cardinalities. Methods such as the Maximum Mean Discrepancy (MMD) and the Wasserstein distance offer promising solutions by treating these sets as samples from distributions, enabling the comparison of sets with different sizes and structures [55]. For instance, the MMD-based kernel has shown strong performance in adapting to the geometric properties of underlying functions, making it a robust choice for surrogate modeling in complex engineering problems [145]. However, such methods are not structure-specific and may struggle with high-dimensional data or scenarios with significant missing information, underscoring the need for more specialized kernels that can effectively capture the underlying structure and relationships within the data.

In the complex systems architecting context, the works [31, 32, 35] detail the Architecture Design Space Graph (ADSG) and its application for modeling complex architectural designs spaces with a semantic approach. In this approach, three types of architectural decisions are available: function-component mapping, component characterization, and component connection. The graph model is constructed from a design space definition, and discrete architectural decisions are automatically inserted according to specified rules. The DSG abstracts away from the system architecture context, and uses a directed graph to model general-purpose hierarchical selection choices (*i.e.*, selections between mutually-exclusive options) and connection choices (*i.e.*, connection patterns between sets of source and target nodes). The current work integrates the architectural decisions of the DSG, notably for automatic construction of the domain in the software part of this work. However, the DSG supports cyclic graphs and therefore includes but is not limited to DAG. A notable tool in this domain is `ConfigSpace` [92], an open-source Python library that facilitates the definition and management of hierarchical design spaces. `ConfigSpace` supports mixed-discrete variables, conditional activation of design variables, and value constraints. It allows for querying and validating design vectors, correcting and imputing design vectors, and generating valid design vectors. It is widely used by surrogate modeling and optimization frameworks such

as SMAC3 [92], BOAH [91], OpenBox [77], and SMT [135]. Even if explicit hierarchical models are not available, problems often contain some implicit hierarchical structure [33]. Various design space modeling techniques, including the Architecture Decision Graph [142], the Adaptive Reconfigurable Matrix of Alternatives [98], or the aforementioned DSG to cite a few, provide useful frameworks for understanding and optimizing complex systems. More relevant background on data representations within structured spaces is given in [Appendix A](#).

### 2.2.2. General distances over structures

One of the objectives of this paper is to propose a distance to compare two hierarchical input points and to build a correlation kernel on top of such distance. The goal of this section is to give more insights on these particular domains. To begin with, recall that a function  $d$  is called a distance if and only if  $d$  respect the four criteria of positivity (1), identity (2), symmetry (3) and respects the triangular inequality (4). In particular, when a function only respects the points 1, 3 and 4, it is called a pseudo-distance and when it only respects the points 1, 2 and 4, it is called a quasi-distance [52].

Another closely related concept is the similarity  $s$  [67] defined as a function that respects the boundness (instead of positivity), identity, symmetry and respects the triangular inequality. However, several authors do not include the symmetry in the definition of the similarity measure [151] while some authors add the positivity but remove the triangular inequality [107]. Furthermore, some authors introduce dissimilarity measures that respects only positivity and reflexivity (instead of identity) and divergence measures that respect both positivity and identity [49]. Therefore, distances must be preferred over similarity distances. Most definitions of similarity measures include correlation and, for example, the Pearson’s R correlation [25] is bounded, symmetric and respects the identity, but not the positivity and the triangular inequality [43]. This is the case with most correlation similarities (e.g., distance correlation, Rho-vectorial coefficient [125], Brownian covariance [148], polychloric correlations [47]).

Both distances and similarity measures can be distinguished according to their deterministic or stochastic nature. For example, distances between vectors includes Minkowski and Mahalanobis distances, generalizing Euclidean distances [27] in, respectively, a deterministic and a stochastic setup. General objects could also be compared with respect to precise features they have. For example, the cosine similarity (Otsuka–Ochiai coefficient) [146] is a measure between vectors with respect to the angle that they form. Distances tend to form families of distance and to rely on parameters and thus, are connected to the fields of hyper-parameters optimization, feature selection and metric learning. More details about common distances are given hereinafter.

In the previous section, we mentioned the EMI [63] measure that extends Jaccard similarity index, and Tanimoto measure [60, 64] to compare generic variable-size vectors or deterministic sets [152]. Similar literature worth noting includes several basic distances over non-structured set. Among other, we can cite the Hamming distance [73], Morisita’s overlap index [36], Szymkiewicz–Simpson coefficient [129], Renkonen similarity index [123], Dice–Sørensen index [144], Lee–Mannheim distance [104] or Tversky index [151].

Distances between strings or sequences can be measured using various probabilistic or deterministic methods. For time-series, deterministic approaches include resampling followed by Minkowski or cosine distances [84], frequency-based features like Fourier transforms [3],

and elastic measures such as time-warped edit distance [96]. Stochastic approaches often rely on auto-regressive models [138], such as using Kullback-Leibler divergence between Markov chains as a Bayesian similarity measure [120], or the Wasserstein-Fourier distance for stationary series [38]. For ordered data, rank-based metrics like Kendall’s Tau and Spearman’s Rho [95] compare element ranks instead of values. More generally, information-based measures like Kolmogorov complexity can be approximated by the normalized compression distance [46]. Simple distances can also be extended to hierarchical data, from sets [11] to more complex structures discussed in the next section.

### 2.2.3. Graph-based distances to compare structured data

Graph representation is amongst the most popular hierarchical database representation even if not the only solution to model such hierarchies. However, it is the most appropriate to our context of hierarchical variables for architectural problems (see [Appendix A](#) for more background information). In fact, rather than comparing individual decision variables, these methods treat each architecture as a complete graph and quantify similarity through operations such as edge insertion, deletion, and permutation-based alignment of shortest-path or adjacency matrices. By focusing on holistic graph topology, this alternative approach captures structural differences and commonalities in hierarchical designs, complementing variable-level metrics with a well-established graph-similarity perspective. Various methods measure similarity or distance between elements in hierarchies and taxonomies, categorized by feature-based [108], morphism-based [154], or structural properties, including deterministic and stochastic distances.

Deterministic distances, like Rada’s distance [118], compute the distance in a hierarchy by counting edges up to the Lowest Common Ancestor (LCA). The LCA distance [18] measures the path length between two nodes starting from their common ancestor, with the idea that nodes with a more specific common ancestor are more similar. Path distance also fits into this category, as it measures the length of the path between two nodes, often considering their depth or level in the hierarchy [157]. Rada’s distance is defined as:

$$d_{\text{Rada}}(\mathbf{X}, \mathbf{X}') = \text{path}(\mathbf{X}, \text{LCA}(\mathbf{X}, \mathbf{X}')) + \text{path}(\mathbf{X}', \text{LCA}(\mathbf{X}, \mathbf{X}')),$$

where  $\text{LCA}(\mathbf{X}, \mathbf{Y})$  represents the lowest common ancestor of  $\mathbf{x}$  and  $\mathbf{y}$  in the hierarchy.

Stochastic distances, such as Resnik’s distance [124], introduce the use of information content (IC) to measure similarity, based on the probability of encountering concepts and their hierarchical significance. Resnik’s distance is defined as:

$$d_{\text{Resnik}}(\mathbf{X}, \mathbf{X}') = -\log(p(\text{LCA}(\mathbf{X}, \mathbf{X}'))).$$

Hybrid distances, e.g., Jiang-Conrath distance [78], combine edge counting and IC for a more comprehensive measure. Additionally, in the realm of stochastic approaches, Wasserstein-based distances, like the Sliced Wasserstein Weisfeiler-Lehman (SW-WL) kernel [37], provide a powerful framework for measuring structural similarity between meshes. These distances are commonly used in transport theory to compare distributions over graph features. These approaches are also useful when working with non-attributed graphs and enable the efficient computation of graph distances using multi-level refinements of graph structure [103].

Graphs are powerful tools for representing hierarchical structures, especially for heterogeneous data. Graph Edit Distance (GED) [61] is widely used to quantify the similarity between two graphs by calculating the minimal cost to transform one graph into another through edit operations like node and edge insertions, deletions, or substitutions. GED generalizes several similarity measures, such as Hamming and Jaro-Winkler distances [156]. It satisfies properties like non-negativity, identity, symmetry, and the triangle inequality [139]. The computation of GED depends on the type of graph considered. For attributed graphs, similarity is based on node and edge attributes [21], with approaches including self-organizing maps [101], and graph kernels [102]. For non-attributed graphs like directed acyclic graphs or trees, GED can be computed using string-based methods, such as tree edit distance, which takes advantage of polynomial-time tree isomorphism problems [57]. Methods like Dijkstra’s algorithm [127] are often more efficient for these cases. These methods convert graphs into strings and compute the shortest edit path using algorithms such as Dijkstra’s or maximum *a posteriori* (MAP) [126], which avoid matrix normalization to reduce complexity.

In addition to graph edit distance, one can measure similarity by aligning global matrix representations of the graphs. Let  $A_{\mathbf{X}}$  and  $A_{\mathbf{X}'}$  be the adjacency matrices of graphs  $G_{\mathbf{X}}$  and  $G_{\mathbf{X}'}$ , respectively, and let  $D_{\mathbf{X}}$  and  $D_{\mathbf{X}'}$  denote their corresponding shortest-path distance matrices. A family of permutation-based distances seeks a permutation matrix  $P$  that best aligns these representations under the Frobenius norm. For instance, the *chemical distance* [87] is

$$d_{\text{Chem}}^{P_n}(G_{\mathbf{X}}, G_{\mathbf{X}'}) = \min_{P \in P_n} \|A_{\mathbf{X}} P - P A_{\mathbf{X}'}\|_F,$$

where  $P_n$  is the set of all  $n \times n$  permutation matrices and  $\|\cdot\|_F$  denotes the Frobenius norm, selecting the node alignment that minimizes adjacency discrepancies. Likewise, the Chartrand–Kubiki–Shultz (CKS) distance [42] applies the same principle to shortest-path information,

$$d_{\text{CKS}}^{P_n}(G_{\mathbf{X}}, G_{\mathbf{X}'}) = \min_{P \in P_n} \|D_{\mathbf{X}} P - P D_{\mathbf{X}'}\|_F,$$

emphasizing global connectivity differences. Other related measures include Poole’s most interesting common generalization distance [115], which abstracts both graphs to their least general common ancestor before measuring edit cost, and the Champin–Solnon mapping cost [39], which allows flexible (non-bijective) vertex correspondences via a cost matrix. Wang and Ishii’s formulation [155] unifies both adjacency- and path-based distances under the same permutation framework, highlighting the versatility of Frobenius-norm alignment for capturing holistic graph similarity but these distances are related to the graph isomorphism problem [68], making their computation challenging.

This review introduced key concepts and relevant works, identifying a critical gap: the lack of a unified framework or software for handling mixed-variable and hierarchical challenges in complex system design such as architecture design. The following section shows how to extend and generalize further the frameworks introduced in this section with application to surrogate modeling.

### 3. A unified framework for hierarchical design spaces

This section presents a unified graph-based framework to model structured design spaces with mixed variables, hierarchical dependencies, and custom distances, enabling the han-

ding of structured data representations in architectural modeling and optimization [31, 20]. Specifically, excluded variables offer valuable information for computing similarity measures between points that do not share the same variables. This approach enables hierarchical and mixed discrete variables to be effectively incorporated into a correlation kernel or distance metric, facilitating comparisons between architectural configurations. Such correlation kernels belong to the family of graph-induced kernels [119], which are frequently employed in Bayesian Optimization (BO) [90] for heterogeneous datasets, making them a powerful tool for managing complex, structured design spaces [81].

### 3.1. Adding relationships in-between variables

In this section, we introduce the new relationships between the variables and their levels in the graph-structured design space that is a hierarchical domain equipped with a graph structure modeling the hierarchical dependencies between the variables. In particular, we introduce these three new relationships.

*Decree dependencies.* This is the most general meta to decreed relationship between any two variables, capturing multi-level and nested inclusion or exclusion dependencies as detailed in Section 2.1.1. To be more precise, we introduce *partially-decreed* variables for when a parent does not fully enable or disable its child, but rather restricts the child’s admissible values without entirely excluding it. For the toy example in Figure 2, the number of motors per wing  $m$  is a meta variable parent of the number of propellers  $p_1$  and  $p_2$ , since it controls their inclusion or exclusion. The variable  $m$  is also a meta variable parent of the length of wings  $l$  since it determines its admissible values. The variable  $l$  is partially-decreed, since it is always included, but its admissible values are controlled by  $m$ .

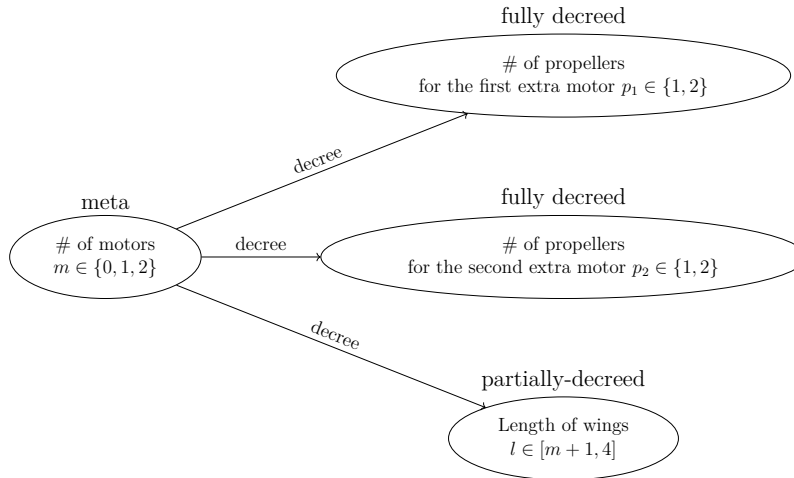


Figure 2: Variables roles for aircraft design problem.

*Incompatibility.* An incompatibility relationship, similar to the “Excludes” constraint in feature models (Section 2.1.3), prevents two variables from taking certain combinations of values. For instance, a specific battery type may be incompatible with high fuel levels for hybrid energy due to safety concerns as in Figure 3. *Mandatory* constraints can also be captured

indirectly: if selecting a value excludes all but one option of another variable, the remaining option becomes implicitly required, effectively modeling a “Requires” relationship.

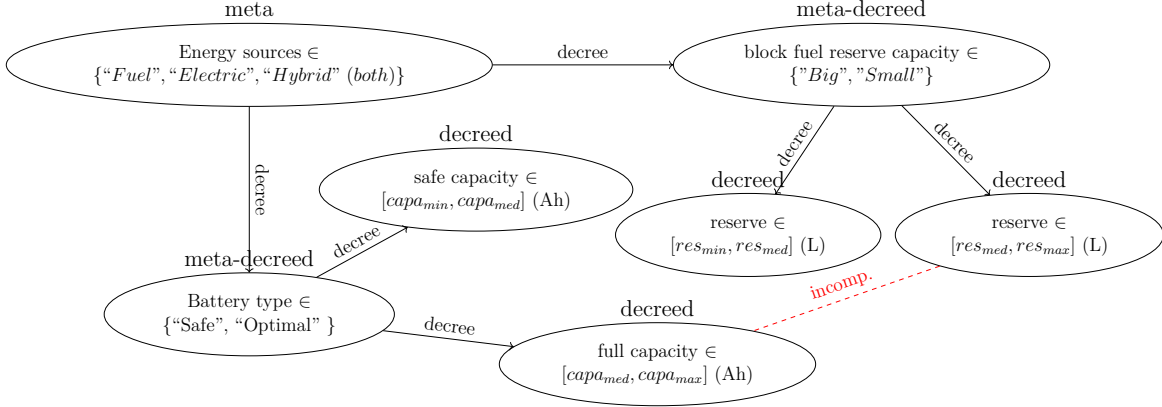


Figure 3: Variables roles for aircraft design problem.

*Order relationship.* For continuous variables, whose supports cannot be enumerated, incompatibilities are expressed through order relations (e.g., inequalities). Equality constraints can, similarly as before, be constructed from the conjunction of two opposite inequalities, enabling *Mandatory* relationships in a continuous setting. For instance, in designing a hydrogen tank, if there are three pressure variables such that  $P_{min} < P_{input} < P_{max}$  [111], this relationship holds true with Figure 4 structure.

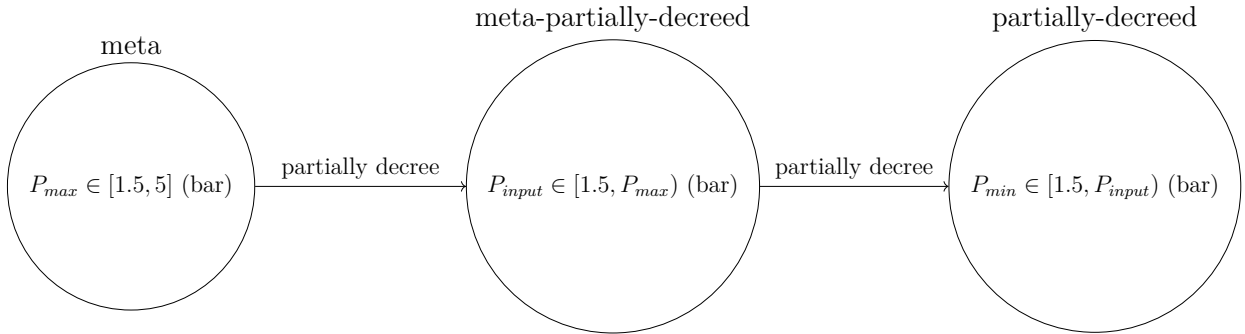


Figure 4: Roles of variables for a pressure order example.

We can go even further by mixing categorical variable and partially-decreed continuous bounds. A dummy example inspired from [58] is as follows. The energy used for propulsion could be either “Fuel”, “Electric” or “Hybrid” (both fuel and electricity). If the energy is either electric or hybrid, a back-up battery needs to be sized but if the energy is hybrid and the fuel reserve is sufficient, no back-up battery is needed. Therefore, the back-up battery capacity is a decreed variable that is included if the energy is electric or if the energy is hybrid but the reserve is too small. To model the “and” interaction, an “intermediate node” as shown in Figure 5, needs to be added to the model. The intermediate variable is decreed by the energy variable and is included only if the source is hybrid electric and its value is 1 if the fuel reserve is insufficient and 0 otherwise. The backup battery is included if the intermediate value is included and of value 1 or if the energy source is electric.



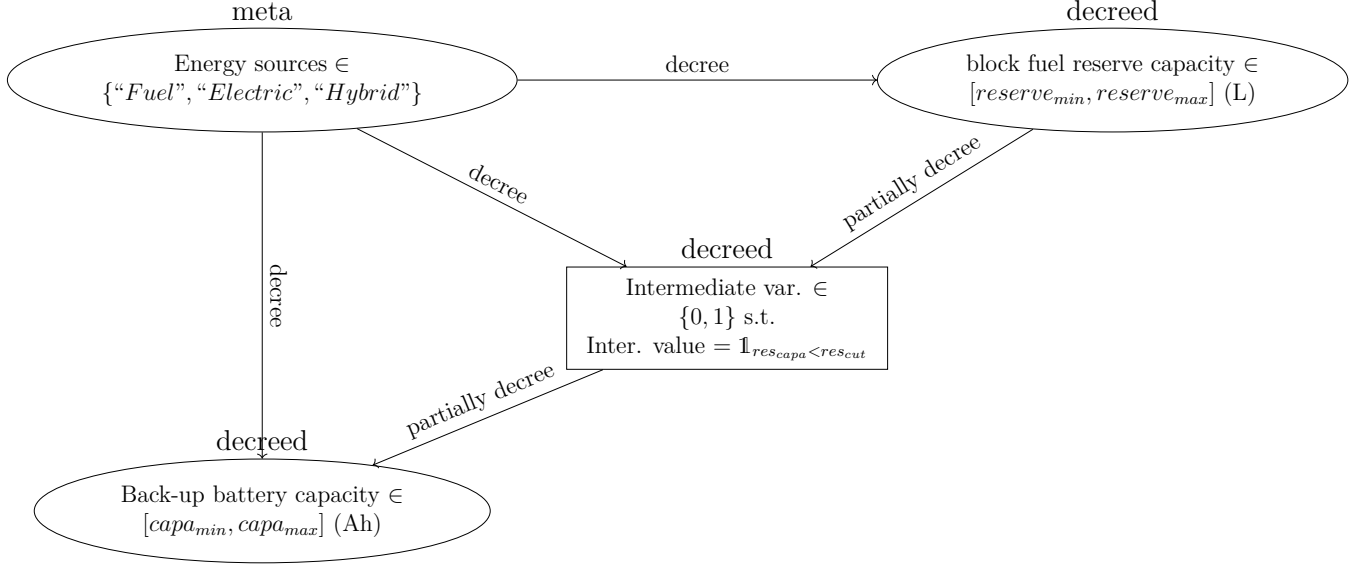


Figure 5: Roles of variables for a hybrid-electric technology choice example.

This work extends the notion of variable roles to accommodate a wider range of applications, including aerospace system design [34, 35, 142] and software architecture [4]. Unlike traditional feature models, our representation is a DAG rather than a tree, allowing features to have multiple parents. The framework is more formally described in the following section.

### 3.2. Generalizing the hierarchical definition

Compared to the previous work [72], we extend the graph to include more concepts and have a structure that is more complex but more flexible and more general. This new structure adds the novel concepts developed in the previous section and is partly inspired by feature model and graph theory concepts. Consequently, it is not a plain directed graph  $(N, A)$  but a so-called mixed graph  $(N, A, E)$ , that mixes arcs  $A$  and undirected edges  $E$ . Notwithstanding, we limit our work to graphs that are directed and acyclic if we do not consider the undirected edges.

**Definition 1** (Generalized role graph). *The generalized role graph  $\mathcal{G} = (N, A, E)$  is a graph structure, where*

- *$N$  is the set of nodes that contains 1) all the included and excluded variables, together with their levels if discrete or bounded supports if continuous, and 2) all intermediate variables,*
- *$A$  is the set of decree dependencies that contains references for all inclusion-exclusion or admissible values dependencies between two nodes, represented as arcs,*
- *$E$  is the set of incompatibilities that contains references for all incompatibilities between two nodes, represented as edges.*

A node  $n \in N$ , which refers to any variable or support, can be of three possible kind:  $N = N_{var} \cup N_{levels} \cup N_{bnd} \cup N_{mid}$  where  $N_{var}$  is the set of possible variables,  $N_{levels}$  is the set of the



levels of any discrete variable,  $N_{bnd}$  is the set of continuous bounds for any continuous variable and  $N_{mid}$  is the set of intermediate nodes modeling composite (e.g. “and/or”) activation conditions. Likewise features in features model in Section 2.1.3, a node is more general and not limited to a variable.

An arc  $a \in A$ , which refers to any dependency, connects a parent (variable) to a child (variable), whose inclusion or admissible values are influenced by the parent or to a child (level/bounds) that is part or the complete support of the variable. We then have  $A = A_{dec-met} \cup A_{bnd-lim}$  where  $A_{dec-met}$  is the set of meta/decreed relationships,  $A_{bnd-lim}$  is the set of partially meta/decreed relationships.

An edge  $e \in E$  which refers to any incompatibility, can be of two kinds  $E = E_{opposed} \cup E_{order}$  where  $E_{opposed}$  is the set of completely incompatible two nodes and  $E_{order}$  is the set of order relationships between two variables.

As in Section 2.1.1, a variable is assigned one type and one role. Their types are continuous (cont), ordinal (ord), integer (int), or categorical (cat) as explained in Section 2.1.1. In particular, ordinal variables are intermediate variables that can be either integer such as  $\{2,4,8\}$  or categorical such as  $\{\text{small}, \text{medium}, \text{high}\}$  but with an order relation ( $\text{high} > \text{medium} > \text{small}$ ) and are therefore quantitative (qnt) like integer or continuous variables. Variables also come with bounds or support/levels definitions. The role is amongst meta (m), meta-decreed (md), decreed (dec) or neutral (neu).

In this framework, each node can have parents that are the other nodes in  $N$  that directly influence its activation or admissible values. A node’s parents are simply those connected to it by a directed arc in the graph. These node parents must themselves be included (*i.e.*, not excluded from the design). To handle the heterogeneous design space, we extend each point to include all possible dimensions, enabling direct comparisons between them—a strategy formally validated in [72], which relies on the notion of support as a variable admissible values depends on its parent values. The support, knowing the role graph  $\mathcal{G}$ , is defined as follows:

**Definition 2** (Support). *Let  $x_i$  be a variable with full value space  $\mathcal{X}_i$  and let  $P_i \subset N$  be the set containing its parents in the graph  $\mathcal{G}$ . The support of  $x_i$ , that depends on the values taken by its parents, is written as  $\mathcal{S}_{\mathcal{G}}(x_i \mid P_i) \subseteq \mathcal{X}_i$  or  $\mathcal{S}_i \subseteq \mathcal{X}_i$  for short. This support is the set of admissible values that  $x_i$  can take under the design space graph  $\mathcal{G}$  and the values taken by its parents. A variable is considered excluded from the design space when  $\mathcal{S}_{\mathcal{G}}(x_i \mid P_i) = \emptyset$ .*

In fact, a variable could be excluded, and in that case its support is the empty set, but it also could be partially included, and in such case its support is a subset of the full support. This leads to the following definition of a partially-decreed variable, a variable that is always present, but whose admissible values are constrained by the values of its parent.

**Definition 3** (Partially-decreed variable). *A variable  $x_i$  is said to be partially-decreed by its parents  $x_j \in P_i$ , if*

$$\mathcal{S}_{\mathcal{G}}(x_i \mid x_j) \subset \mathcal{X}_i \quad \text{and} \quad \mathcal{S}_{\mathcal{G}}(x_i \mid x_j) \neq \emptyset.$$

*This generalizes the decree logic [8]: if  $\mathcal{S}_{\mathcal{G}}(x_i \mid x_j) = \mathcal{X}_i$ , then  $x_i$  is fully included (conditionally included); if  $\mathcal{S}_{\mathcal{G}}(x_i \mid x_j) = \emptyset$ , it is excluded (conditionally excluded).*

The source-to-target assignment problem features such variables [32]. In that problem, either 1 or 2 consumers are assigned to either 1 or 2 energy sources. Two hierarchical interactions arise: if there is only one source, then both consumers have to be assigned to that source, and if there is only one consumer, the source choice for the second consumer is not included. Figure 6 illustrates the roles of variables for this source-to-target example. This problem includes 4 variables: the number of energy sources between 1 or 2, the number of consumers between 1 or 2, the source of energy used by the first consumer and the source of energy used by the second consumer. There is 4 meta possibilities: if 1 source and 2 consumers, the assignment variables are partially-decreed because only the possibility “source number 1” can be chosen. If 2 sources and 2 consumers, the assignment variables are fully decreed, both “source number 1” and “source number 2” are available for both consumers. If 2 sources and 1 consumer, the variable “source of energy for the first consumer” is fully decreed but the variable “source of energy for the second consumer” is completely excluded because there is no second consumer, in that case, the only possibility for that variable is “no possibilities” or empty set. If 1 source and 1 consumer, the variable “source of energy for the first consumer” is partially-decreed but the variable “source of energy for the second consumer” is completely excluded. As shown by this example, a same variable can be either partially or completely decreed depending on the problem and meta variable. Therefore, contrarily to other roles, partially-decreed and decreed property are not mutually exclusive roles and as such, we may also consider meta-partially-decreed variables, that is variables that are both meta and partially-decreed. In particular, if a meta variable prohibits a value of another meta-partially-decreed variable, and if this value was decreeing another variable, then, the first meta variable is in fact excluding the latter variable: nested variable can create complex graph relations.

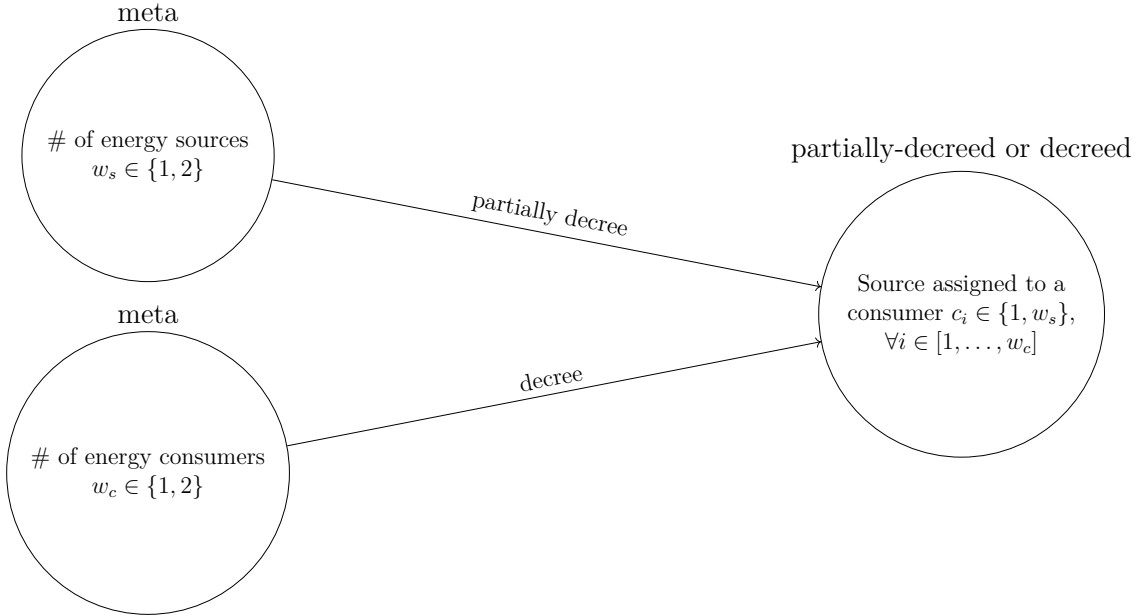


Figure 6: Roles of variables for a source-to-consumer example.

However, in our novel extended framework, it is possible to have completely incompat-

ible variables and therefore we need to be able to compare two points without any choice-dependence. The latter remark excludes some classical approaches to compare heterogeneous data such as the imputation method [32]. Consequently, in the next section, we will show how to construct a well-behaving distance and kernel to deal with mixed hierarchical points.

### 3.3. Mixed hierarchical kernels for hierarchical domains

SMT 2.0 introduced a hierarchical correlation kernel that accounts for both meta and decreed variables, and was further extended in [130] to handle distances between decreed continuous variables. In this work, we generalize the SMT framework to support fully hierarchical domains. This extension enriches the `DesignSpace` definition with support for meta-decreed, partially-decreed, and order-based relationships, as described in this section<sup>3</sup>. With these variable types and structural relations, we can now define a generalized design space suitable for hierarchical surrogate modeling.

**Definition 4** (Graph-structured design space). *The design space  $\mathcal{X}$  represents the set of all possible and admissible configurations of variables based on the graph  $\mathcal{G}$ . Each point  $\mathbf{X} \in \mathcal{X}$  is a configuration defined by a tuple of variable values  $(X_1, X_2, \dots, X_n)$ , with  $X_i$  is the value of  $\mathbf{X}$  for the  $i$ -th variable  $x_i$ , and it may include continuous, discrete, or categorical variables.*

The span of the design space is the Cartesian product of the supports of the variables possibly included within it, where we define a distance function

$$d_i : \mathcal{S}_i \times \mathcal{S}_i \longrightarrow \mathbb{R}_+,$$

The function  $d_i(X_i, X'_i)$  is defined as:

$$d_i(X_i, X'_i) = \begin{cases} d(X_i, X'_i), & \text{if } X_i, X'_i \in \mathcal{S}_i, \\ \delta_i, & \text{if exactly one of } X_i, X'_i = \emptyset, \\ 0, & \text{if } X_i = X'_i = \emptyset. \end{cases} \quad (1)$$

where  $d$  is any 1-dimensional distance function (see Section 2.2.2) and where  $\delta_i = \max\{d(X_i, X'_i) : X_i, X'_i \in \mathcal{S}_i\}/2 \geq 0$  is constant ensuring the triangular inequality is respected between included and excluded variables, as proven in [72]. Note that a particular case of the proof for  $\delta_i$  is given in Appendix D. Finally, for any  $p \geq 1$ , the hierarchical function  $\text{dist}_p : \mathcal{X} \times \mathcal{X} \rightarrow \mathbb{R}^+$  defined by

$$\text{dist}_p(\mathbf{X}, \mathbf{X}') := \left( \sum_{i=1}^n d_i(X_i, X'_i)^p \right)^{1/p}. \quad (2)$$

In [62], the authors found good results with kernels approaches because “Unlike the traditional edit distance, kernel functions makes good use of statistical learning theory in the inner product rather than the graph space directly”. Therefore, this work was motivated by the need to extend graph distances to handle mixed hierarchical variables. We generalize

---

<sup>3</sup>[https://smt.readthedocs.io/en/latest/\\_src\\_docs/applications/Mixed\\_Hier\\_usage.html](https://smt.readthedocs.io/en/latest/_src_docs/applications/Mixed_Hier_usage.html)

the SMT 2.0 hierarchical kernel as the product of three Symmetric Positive Definite (SPD) sub-kernels: a neutral kernel for variables without dependencies, a meta kernel for high-level configuration choices, and a meta-decreed kernel that ties each choice to its activated children via our graph-distance. Because each factor is SPD, their product is SPD as well, and the resulting kernel naturally handles mixed variable types, conditional activations, and hierarchical structure. More details and the SPD proof are given in [Appendix D](#). Also, in this work, we will use the so-called algebraic distance introduced in [\[130\]](#), namely

$$d(\mathbf{X}, \mathbf{X}') = \begin{cases} 1, & \text{if } \mathbf{X}^\top \mathbf{X}' = 0 \\ \frac{\|\mathbf{x} - \mathbf{x}'\|}{\sqrt{\|\mathbf{x}\|^2 + 1} \sqrt{\|\mathbf{x}'\|^2 + 1}}, & \text{otherwise.} \end{cases} \quad (3)$$

This distance is well-defined as proven in [\[72\]](#) and the kernel that results from such distance, known as the Alg-Kernel is SPD as proven in [Appendix D](#). This distance is a particular case of the more general hierarchical distance introduced in [\[72\]](#).

#### 4. Surrogate modeling and Bayesian optimization with graph-structure inputs

In this section, we will connect the implementations of the mixed hierarchical surrogate models with the graph-structured design space. In particular, we will describe the method implemented in SMT to build a hierarchical GP and show an illustration on the hyperparameters optimization of a neural network (see [Appendix B](#)) and an application to a green aircraft optimization through BO.

##### 4.1. The architecture graph-structured design space implementation and usage

Here we extend the framework from [\[135\]](#) by incorporating the key features reviewed in [Section 2](#). Our implementation builds on SMT 2.0’s design-space tools [\[135, 23\]](#), the ConfigSpace library [\[92\]](#), and the DSG of the software Architecture Design Space Graph `adsg-core` [\[31, 30\]](#), making it practical for real-world use<sup>4</sup>. [Table 1](#) outlines the main features of the Python modeling software that can handle hierarchical and mixed variables within SMT, chosen within the open-source software literature based on its mixed variable handling capacities as detailed in [\[135, Table 1\]](#) where several are compared for such modeling task. The default option in SMT is a basic DSG that is limited to one level of hierarchy and is not able to handle complex relationship such as incompatibility constraints even if hierarchical. The ConfigSpace design space may be slow and is not based on the graph structure. Overall, the best option for architecture modeling is the DSG of the `adsg-core` toolbox that is fast and gives explicit visualizations of the DSG in DOT language [\[53\]](#) and our main software contribution has been combining AD SG to work within SMT to define hierarchical surrogate models.

---

<sup>4</sup><https://adsg-core.readthedocs.io/en/latest/>

Package	License	SMT interface name	Mixed hier. var.	Nested hier.	Incomp. (excl.)	Graph struct.	Explicit & visu.
SMT [135]	BSD	DesignSpace	✓	–	–	✓	–
ConfigSpace [92]	BSD	ConfigSpaceDesignSpaceImpl	✓	✓	✓	–	–
adsg-core [31]	MIT	AdsgDesignSpaceImpl	✓	✓	✓	✓	✓

Table 1: Comparison of software packages for hierarchical and mixed design-space definition.

We can automatically define a DSG from the variables specifications<sup>5</sup>. The DSG models hierarchical choices using selection and connection choice nodes, that select between mutually exclusive option nodes and connect sets of source nodes to targets nodes, respectively [31]. Nodes are subject to selection and only obtain meaning in the context of an optimization problem. Its original context was function-based modeling of system architecture design spaces, called the Architecture Design Space Graph (ADSG), where various types of nodes such as functions, components, and ports, were defined.

For illustrating the method, let `design_space` be the SMT 2.0 `AdsgDesignSpaceImpl` defined in Appendix C (Figure C.12) for the Multi-Layer Perceptron (MLP) problem. In a DSG, both neutral and purely meta variables serve as graph roots, also referred to as “permanent nodes” or “start nodes,” while decreed and meta-decreed variables function as “conditional nodes.” A choice that depends on a meta or meta-decreed variable is represented by a choice node (in blue) and is connected to the variable name and its possible choices through derivation edges. Future work may include automated formal verification of the graph structure. However, some verification steps are already handled within the DSG. For instance, the DSG is considered infeasible if an incompatibility edge is defined between two permanent nodes, ensuring that conflicting configurations are detected early. To do this, the *encoder* maps architectural choices, such as selections and connections in the graph into a numerical design vector  $\mathbf{x}$  that optimizers can handle. Therefore, selection and connection choice encoders enable a full enumeration of valid design vectors, and ensure any source-to-target connection problem can be encoded such that optimization algorithms can effectively search the design space. The encoder plays a crucial role in mapping selection choices from the hierarchical space to discrete variables in the input vectors, ensuring correct associations with input points for tasks such as sampling. Currently, two encoding methods are implemented. The *complete encoder* performs an exhaustive exploration of the design space, identifying all valid configurations and providing accurate imputation ratios. In contrast, the *fast encoder* offers a more efficient but less comprehensive approach by directly mapping selection choices to design variables. While the fast encoder significantly reduces computation time, it may overlook some valid configurations, making it more suitable for large design spaces with computational constraints.

To construct the DSG shown in Figure 7, we only need to define the variables, levels and relationships. Then, the DSG is processed to have a visual graph with the nodes in  $N_{\text{var}}$  in blue if categorical and white otherwise, the nodes in  $N_{\text{levels}}$  in white and those in  $N_{\text{bnd}}$  in straw color. The edges in  $N_{\text{opposed}}$  are colored in red. The DSG also automatically processes the graph to generate outputs, as presented in Table 2.

<sup>5</sup><https://github.com/SMTorg/smt-design-space-ext/>

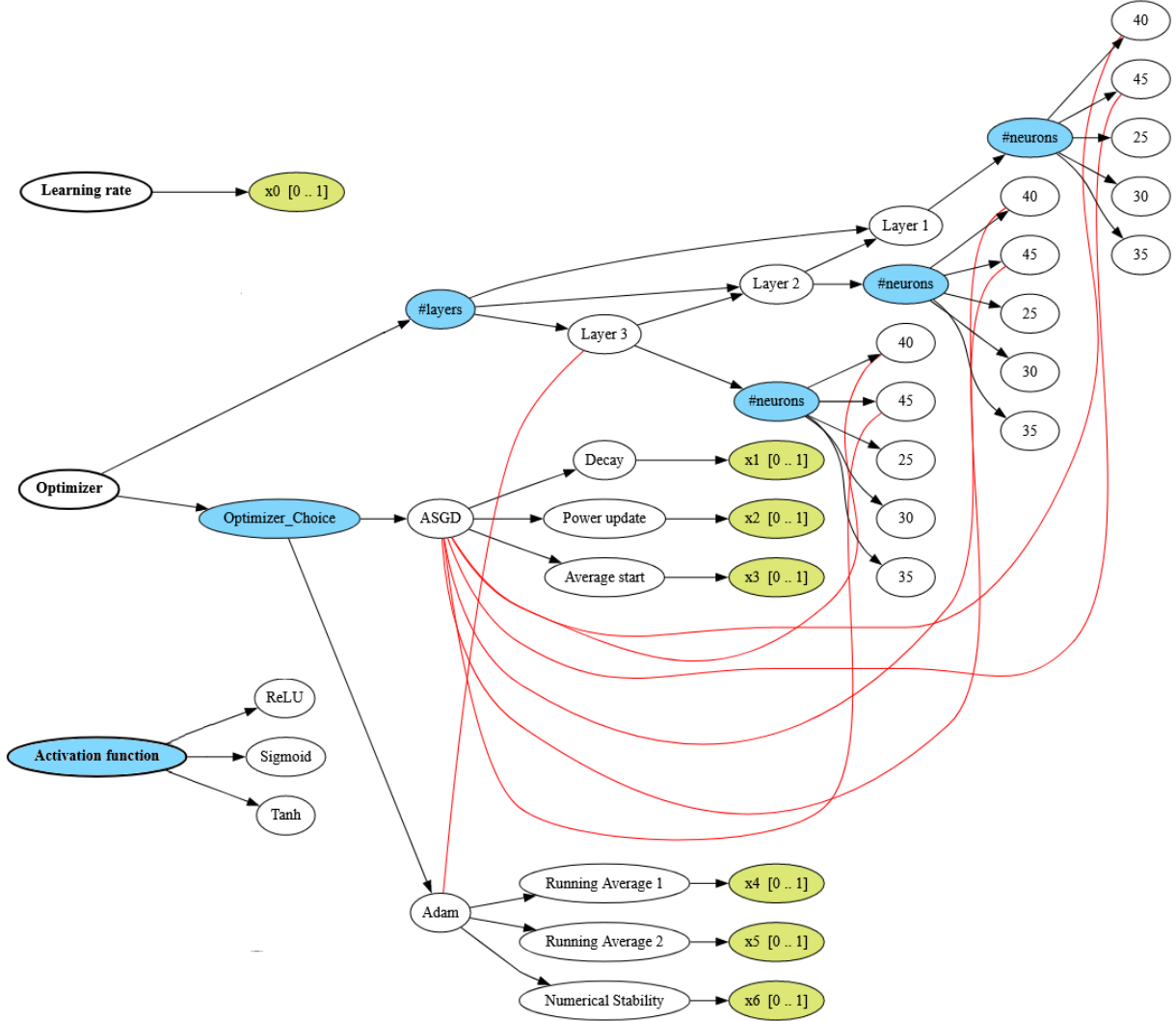


Figure 7: DSG definition for the neural network problem.

Type	n_valid	n_declared	n_discrete	n_dim_cont	n_dim_cont_mean	imp_ratio	encoder
option-decisions	207	1350	6	0	0.0	6.521739	complete
additional-dvs	207	0	0	7	4.0	1.750000	
total-design-space	207	2250	6	7	4.0	10.869565	complete

Table 2: Processed DSG on the neural network problem.

This analysis provides useful insights, including the imputation ratio, which measures the ratio between the total number of declared categorical and integer possibilities and the number of feasible instances. In this case, 2250 possibilities are declared, but only 207 are valid, meaning that approximately 1 in 10.9 instances is feasible. The table also displays the total number of variables, which consists of 13 variables—6 discrete and 7 continuous. The continuous imputation ratio is 1.75, indicating that only 4 out of the 7 continuous variables are included. Specifically, the included variables correspond to either the combination of “decay,” “Power update,” and “Average start” or the combination of “Running average 1,” “Running average 2,” and “Numerical Stability.” In Table 2, the “encoder” column confirms

that the complete encoder was used for this problem, reflecting a thorough approach in identifying all valid design vectors.

Thanks to the DSG, we can make explicit the definition of the hierarchical model by giving directly the model and generate valid configuration as in Figure 8. This new class upgrades and improved on the prior `ConfigSpaceDesignSpaceImpl` class that did not take into consideration hierarchical spaces. The two can be compared on processing tasks as described in Table 3. The most important task consists in correcting a non-valid input point and returning both a corrected input and its corresponding included variable within the extended space (called active). This task of projecting an input from the extended domain to the hierarchical space is really important since the hierarchical distance is computed on the extended domain and then projected as this projection is an isomorphism [72, Theorem 2]. On this task, we observe, on Table 3 an improvement by 76 % with the `AdsgDesignSpaceImpl` that relies on adsg-core implementation compared to our legacy `ConfigSpaceDesignSpaceImpl` method relying on `ConfigSpace`. Another processing task is enumeration of all discrete possibilities, and in Table 3, we obtained a 36% speed up with the `AdsgDesignSpaceImpl` class for such task. To finish with, one could want to generate a design of experiments that respects the graph-structure domain. On this task, we obtain a 15% improvement with our class, but to achieve this performance, we first generated one random point for each of the 207 possible discrete configurations and then subsampled 100 points from that set: an approach also adopted by `SBArchOpt` [29]. However, one might alternatively choose to sequentially sample additional points. While it is straightforward to parallelize the sampling of 100 points, doing so sequentially is approximately 15 times slower than the subsampling approach.

Class name	Correct and compute activeness of 1000 invalid points	Generate 1 point by discrete possibility (207 points)	Generate 100 valid points
<code>ConfigSpaceDesignSpaceImpl</code>	2.2300s	0.0081s	0.0054s
<code>AdsgDesignSpaceImpl</code>	0.5356s (-76%)	0.0053s (-36%)	0.0046s (-15%)

Table 3: Comparison of processing duration for several tasks with `ConfigSpaceDesignSpaceImpl` and `AdsgDesignSpaceImpl`.

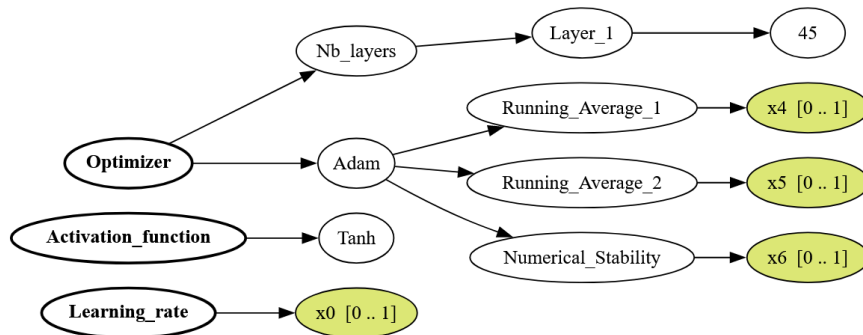


Figure 8: `AdsgDesignSpaceImpl` sampling.

In the next section, we will use the graph-structured design space graph of SMT and AD SG to create surrogate Gaussian processes of hierarchical problems while preserving their structure and apply these models for Bayesian optimization.



#### 4.2. Bayesian optimization

Bayesian optimization has emerged as a highly effective technique for optimizing blackbox functions, particularly when these functions are expensive to evaluate, non-convex, or lack gradient information [59]. Its growing popularity in various fields, from machine learning hyperparameters tuning (HPO) to engineering design, is largely due to its ability to achieve near-optimal solutions with a minimal number of evaluations [45]. At its core, BO builds a probabilistic surrogate model, typically a GP, to approximate the objective function that is being optimized. The surrogate model provides not only predictions of the function’s value at any given point in the search space but also an estimate of the uncertainty associated with these predictions. This uncertainty quantification method is the foundation of BO ability to balance exploration (sampling areas of the search space with high uncertainty) and exploitation (focusing on areas predicted to yield high objective values). The BO process typically starts with a Design of Experiments (DoE) to obtain initial evaluations of the objective function. These evaluations are used to fit the GP model, which is then iteratively updated as new function evaluations are conducted. At each iteration, the next point to evaluate is chosen by maximizing an acquisition function to guide the search towards the optimum as fast as possible.

GP are well suited for Bayesian optimization because they can flexibly represent unknown objective functions via a mean function and correlation kernel. The mean gives a prior estimate while the kernel encodes correlations across the search space, allowing uncertainty quantification and efficient predictions. In this work, we adopt the kernel described in Section 3.3, which balances smoothness assumptions with adaptability to mixed continuous, categorical, and hierarchical inputs. Once the surrogate is set up using SMT’s `DesignSpace` class, defining a design of experiments and instantiating corresponding GP models—complete with graph-structured kernels—becomes a single, streamlined step. The acquisition function is a crucial component of BO, responsible for determining the next point to evaluate. Common acquisition functions include Expected Improvement (EI), Probability of Improvement (PI), Upper Confidence Bound (UCB) or Watson and Barnes 2<sup>nd</sup> criterion scaled (WB2s) [79, 140, 14]. In this work, we will use WB2s that is more smoothed and less multimodal than the other classical criteria, that is tractable and easy to optimize with a local optimizer such as COBYLA [116] and the optimizer SEGOMOE [14].

In many real-world optimization tasks, the design variables span continuous, integer, and categorical types, so standard continuous Bayesian optimization has been extended for them. Categorical inputs use specialized kernels and, for comparison with our method, we use Continuous Relaxation (CR), Homoscedastic Hypersphere (HH) or Gower Distance (GD) to capture categorical correlations, while integer variables employ ordinal-aware, distance-based kernels. High dimensionality compounds the challenge, since modeling accuracy typically requires exponentially more samples. To mitigate this “curse of dimensionality,” dimensionality-reduction methods such as Partial Least Squares (PLS) are integrated into the Gaussian-process surrogate. In particular, Kriging with PLS (KPLS) has recently been generalized to mixed-variable—and even hierarchical—spaces, enabling efficient BO over complex, heterogeneous domains [134].

### 4.3. Application to aircraft design

Once we have defined the surrogate model based on the `DesignSpace` class in SMT, we can directly define both DoE and surrogate models such as GP models while accounting for the hierarchical model. In [135], a GP model has been built for the hierarchical neural network problem and promising results have been obtained, and in [130], the GP has been extended to handle decreed continuous variables and meta-decreed variables. In a previous work, we optimized the Distributed fans Research Aircraft with electric Generators by ONERA (DRAGON) but without considering any hierarchy [136] and an additional goal of this article is to show how our framework can be applied in practice. More particularly, hierarchical GP can be used to perform BO of complex and costly systems as illustrated hereinafter.

The DRAGON baseline configuration is two turboshafts, four generators, four propulsion buses with cross-feed and forty fans. This configuration was selected for the initial study as it satisfies the safety criterion. However it was not designed to optimize aircraft weight. The turboelectric propulsive chain being an important weight penalty, it is of particular interest to optimize the chain and particularly the number and type of each component, characterized by some mixed hierarchical values. The multidisciplinary Design and analysis framework for sizing the aircraft is based on FAST-OAD software [50]. The consideration of the variables related to architecture was revised to take full advantage of mixed variables optimization. Three configurations with different number of electric components were considered, each with their own sizing rules. The default configuration is conserved for the analysis and two new configurations, one with low distribution, the other with high distribution, were created and analysed to establish the sizing rules. The number of motors was to remain an optimization variable as it is an important driver of the propulsive and aerodynamic efficiency of the aircraft but it is constrained by the type of architecture. In this analysis, the number of motors could only be multiple of 4, 8 or 12 depending of the selected architecture. The solution consisted in expending the levels of the categorical variable representing the architecture and assign a specific and valid number of motors to each level. The choice of architecture was originally represented by a categorical variable but thanks to the hierarchical framework introduced in this paper, it now can be treated with hierarchical integer variables. Five constraints need to be accounted for when sizing the aircraft detailed in Table 4.

With the previous categorical modeling, we were solving the constrained optimization problem with 10 continuous design variables and 2 categorical variables with 17 and 2 levels respectively, for a total of 12 design variables. For the optimization, this problem is a hard test case involving 29 relaxed variables and 5 constraints. The definition of the turboshaft layout is given in Table 5 and the definition of the architecture variable is given in Table 6. Now, considering the graph-structured design space, we are solving a constrained optimization problem with 10 continuous design variables, 2 integer variables and 1 categorical variable with 2 levels, for a total of 14 design variables. In Table 4, we put both the problems with and without hierarchical domain in orange and blue respectively, but it is up to the modeling choice; either orange or blue variables are included.

Table 4: Definition of the “DRAGON” optimization problem.

	Function/variable	Nature	Quantity	Range
Minimize	Fuel mass	cont	1	
	<b>Total objectives</b>		<b>1</b>	
with respect to	Fan operating pressure ratio	cont	1	[1.05, 1.3]
	Wing aspect ratio	cont	1	[8, 12]
	Angle for swept wing	cont	1	[15, 40] (°)
	Wing taper ratio	cont	1	[0.2, 0.5]
	HT aspect ratio	cont	1	[3, 6]
	Angle for swept HT	cont	1	[20, 40] (°)
	HT taper ratio	cont	1	[0.3, 0.5]
	TOFL for sizing	cont	1	[1800., 2500.] ( <i>m</i> )
	Top of climb vertical speed for sizing	cont	1	[300., 800.] ( <i>ft/min</i> )
	Start of climb slope angle	cont	1	[0.075., 0.15.] ( <i>rad</i> )
	Total continuous variables		10	
	Turboshaft layout	cat	2 levels	{1,2}
	Architecture_cat	cat	17 levels	{1,2,3, ..., 15,16,17}
	Number of cores	int	1	{2,4,6}
	Number of motors*	int	1	{8,12,16,20, ..., 40}
	*graph-structure dependence to the core value			
subject to	Wing span < 36 ( <i>m</i> )	cont	1	
	TOFL < 2200 ( <i>m</i> )	cont	1	
	Wing trailing edge occupied by fans < 14.4 ( <i>m</i> )	cont	1	
	Climb duration < 1740 ( <i>s</i> )	cont	1	
	Top of climb slope > 0.0108 ( <i>rad</i> )	cont	1	
	<b>Total constraints</b>		<b>5</b>	

Table 5: Definition of the turboshaft layout variable and its 2 associated levels.

Layout number	position	y ratio	tail	VT aspect ratio	VT taper ratio
1	under wing	0.25	without T-tail	1.8	0.3
2	behind	0.34	with T-tail	1.2	0.85

Table 6: Definition of the architecture variable and its 17 associated levels.

Architecture number	1	2	3	4	5	6	7	8	9	10	11	12	13	14	15	16	17
Number of motors	2	2	2	2	2	2	2	2	2	4	4	4	4	4	4	4	4
Number of generator	2	2	2	2	2	2	2	2	2	4	4	4	4	4	4	4	4
Number of cores	8	12	16	20	24	28	32	36	40	8	16	24	32	40	12	24	36

To validate our method, we compare the 8 methods described in Table 7 on the optimization of the “DRAGON” aircraft concept with 10 points for the initial DoE. The first six are categorical kernels with different structures introduced and detailed in [132]. The method “HIER” is the one based on the graph-structure design space and the last “NSGA-II” is an evolutionary algorithm posed as a baseline [51]. PLS which stand for “Partial Least Squares” is a reduced order model detailed in [134]. Concerning the matrix based methods, they are too costly for such problems: HH takes 320h, HH with PLS 3D takes 102h and HH with PLS 12D takes 258h.

Table 7: The various kernels compared for optimizing “DRAGON”.

Name	# of cat. params	# of cont. params	Total # of params	Comp. time
<b>GD</b>	2	10	12	36h
<b>CR</b>	19	10	29	62h
<b>CR with PLS 3D</b>	Not applicable	Not applicable	3	14h
<b>HH</b>	137	10	147	320h
<b>HH with PLS 3D</b>	2	1	3	102h
<b>HH with PLS 12D</b>	2	10	12	258h
<b>NSGA-II</b>	Not applicable	Not applicable	Not applicable	16h
<b>HIER</b>	1	12	13	40h

Figure 9 shows promising results with the hierarchical hierarchical domain. Namely, it is a bit more costly than GD for a better result and in terms of convergence behaviour GD, CR and HIER are highly similar. Note that CR with PLS 3D is faster than HIER for little degraded performance and that CR is the best in terms of convergence but is slightly more costly. In the end, HIER is a really good trade-off for BO.

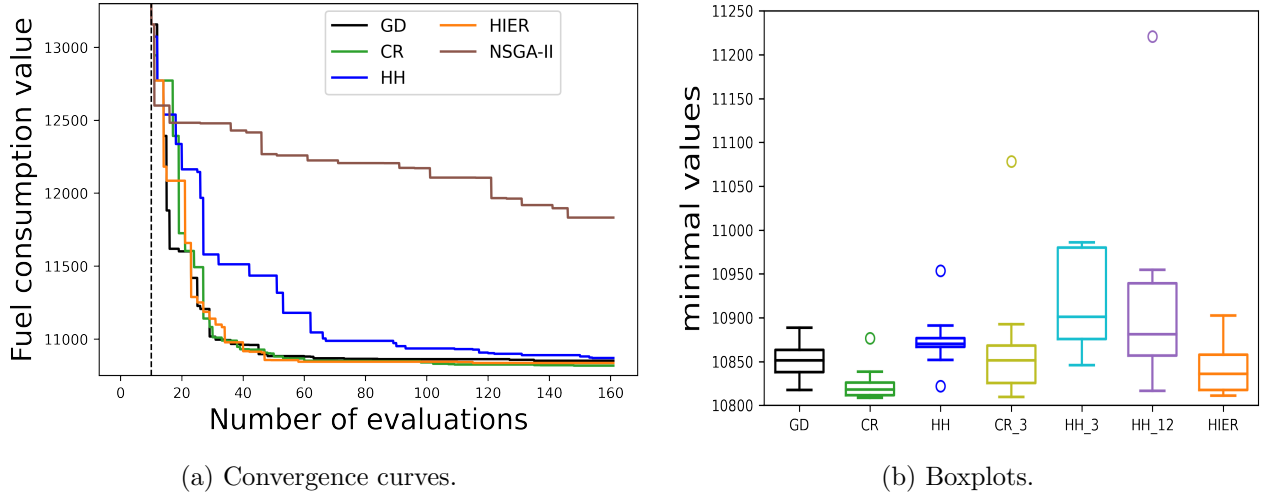


Figure 9: “DRAGON” optimization results using a DoE of 10 points over 10 runs. The boxplots are generated, after 150 iterations, using the 10 best points.

## 5. Conclusion and Perspectives

This work introduced a novel operations research framework designed to define graph-structured design spaces, with application to surrogate modeling and optimization. We built upon previous works, extending their definitions to encompass any DAG, and we enhanced the flexibility and scalability of the framework. Specifically, this work extended the concept of meta and decreed variables presented in earlier research [8, 130], bridging the gap with design space graphs. Afterwards, we demonstrate the improved framework capabilities and we proposed an industrial application to sizing and optimizing complex system architectures [35, 32].

A key contribution of this research is the implementation of the extended framework within the open-source Surrogate Modeling Toolbox software [135]. This open-source toolbox is collaborative and is an easy to use and well documented platform for users and developers. Notably, SMT remains the only open-source toolbox capable of constructing both hierarchical and mixed surrogate models, and it has demonstrated its value in numerous practical applications, such as the optimization of a green aircraft design. In short, this paper lays the groundwork for further developments involving hierarchical models or data. By improving both the theoretical foundation and practical implementation of this framework, the potential applications of this work are vast, ranging from industrial design optimization to more complex systems requiring advanced modeling and optimization techniques.

Several areas of future research and development have been identified. For instance, the new framework still lacks automated formal verification for graph structures. Similar to approaches used in feature models, future work will focus on integrating anomaly detection algorithms to ensure the reliability of the design space [17]. Future research could focus on refining graph structure models and addressing limitations in current methodologies to improve their application in various domains. For instance, the role graph in this work is designed as a DAG to prevent cyclical dependencies, ensuring that meta-decided variables do not influence one another. While DAGs provide clear hierarchical structures and efficient traversal [18], they limit the representation of complex interdependencies. The DSG addresses this by recursively parsing design variables in a flexible, non-linear sequence [31]. Future research will focus on expanding the DSG to incorporate more complex structures, including cyclic dependencies, leveraging advancements like hypergraphs [6] and cyclic graph models [12] to enhance the framework’s applicability to sophisticated optimization and surrogate modeling challenges. However, enumerating all valid instances within such complex structures quickly becomes computationally intractable. To overcome this, advanced operations research techniques will be required to efficiently estimate the number of possibilities and explore these graphs effectively [110]. Another promising direction for future development is the generalization of the framework to enable more automatic learning. For instance, relationships between variables could be learned directly from data [24]. Moreover, adopting more general hierarchical representations could help tackle problems involving partial and incomplete data, particularly when numerous variables exist but are not fully observed [109]. Also we can extend relationships definitions to include any function of the form  $R(\phi(x_1), \psi(x_2))$ .

A further area of interest lies in reducing graph complexity to improve scalability. Future work will explore techniques such as kernelization of the vertex cover problem [28] and propositionalization methods, which convert graph structures into flat propositions, making it easier to apply distance metrics over propositional data [82]. These strategies will enhance the framework’s scalability when dealing with large, complex design spaces. Finally, the framework will be adapted to tackle highly dimensional problems with architectural constraints. This will involve using advanced techniques such as KPLS combined with hierarchical kernels [134, 22]. The goal is to enable the framework to handle more complex optimization tasks by integrating dimension reduction techniques with structural flexibility.

## Fundings

This research is funded by a Natural Sciences and Engineering Research Council of Canada (NSERC) PhD Excellence Scholarship (PGS D), a Fonds de Recherche du Québec (FRQNT) PhD Excellence Scholarship and an Institut de l'Énergie Trottier (IET) PhD Excellence Scholarship, as well as by the NSERC discovery grant RGPIN-2024-05093. This work is part of the activities of ONERA - ISAE - ENAC joint research group. The research presented in this paper has been performed in the framework of the COLOSSUS project (Collaborative System of Systems Exploration of Aviation Products, Services and Business Models) and has received funding from the European Union Horizon Europe program under grant agreement n° 101097120 and in the MIMICO research project funded by the Agence Nationale de la Recherche (ANR) n° ANR-24-CE23-0380.

## Appendix A. Data representation of structured spaces

In general, structured representations can be categorized into three major types: graph-based, logic-based, and frame-based representations [107], although some models fall outside this classification (*e.g.*, general matrices [69]).

Graph-based representations are particularly powerful in fields such as structural pattern recognition and network analysis. In these models, data is represented as graphs, where nodes correspond to entities and edges to the relationships between them. This approach is highly valued for its invariance to transformations, making it robust in various applications where the structure of the data is as important as the content itself [62]. Recent advances in causal representation learning extend these models by approximating latent causal structures from high-dimensional data [24]. This data-driven approach moves beyond correlations and supports out-of-distribution generalization and planning [153, 112].

Logic-based representations are another form of structured representation, widely used in domains such as inductive logic programming and semantic web technologies. These models use logical statements to represent data, enabling complex inferences and generalizations [100]. The key advantage of logic-based representations lies in their ability to encode generalization and inference naturally, allowing for the incorporation of background knowledge through rules. This makes them particularly effective in domains requiring complex reasoning and knowledge representation. For instance, within a data landscape, logic-based representations can show semantic relationships and logical dependencies across different systems or domains, enhancing the ability to spot overarching patterns in knowledge [65]. Horn clauses, description logics, and order-sorted feature structures are key logic-based formalisms. Horn clauses enable software verification and automated theorem proving [5]. Description logics balance expressive power and computational efficiency, sitting between propositional and first-order logic [10]. Order-sorted feature structures, a subset of first-order logic, are used in case-based reasoning and natural language processing [80].

Frame-based representation is a classical approach to knowledge modeling, commonly used in domains like case-based reasoning and Artificial intelligence [99]. Knowledge is organized using attribute-value pairs within a hierarchical structure, where each frame represents a concept or entity. This structure allows properties to be inherited from parent frames, facilitating efficient representation of complex knowledge [143]. Frames also support default values and data types, enhancing their utility in knowledge-based systems [143].



Frames enable reasoning and inference, making them valuable for tasks like automated theorem proving and decision-making [99]. Though similar to other methods like knowledge graphs [83], semantic networks [117], and concept maps [105], frame-based systems remain integral to structured knowledge representation, particularly in case-based reasoning and statistical relational learning [65].

Structured data representations play a crucial role across various domains of machine learning and artificial intelligence, each tailored to the specific demands of different tasks and applications. Recent advances in supervised learning of representations have shown great promise in automatically extracting task-specific features from structured spaces, especially in categorical and graph-based data. These methods not only enhance flexibility but also significantly improve the predictive performance of models [158, 106]. Moreover, supervised learning approaches have been particularly effective in identifying meaningful, task-driven features from complex data structures, offering robust solutions in fields like graph-based modeling and few-shot learning [54, 44]. As research progresses, selecting the appropriate data representation remains a critical factor, as it directly influences the effectiveness of learning algorithms and their ability to generalize across various applications. For example, deep representation learning continues to expand in its ability to handle structured data, which poses unique challenges due to its high dimensionality and inherent complexity [112].

## Appendix B. Modeling a complex MLP system architecture

To illustrate our approach, we introduce a complex system that will be used throughout the paper to illustrate our modeling framework. The Multi-Layer Perceptron (MLP) example provided has been introduced in [8, 72, 141], where an MLP is tuned for a given supervised learning task by optimizing its hyperparameters. Identifying optimal hyperparameters is a problem called HyperParameter Optimization (HPO) that is known to be challenging [66]. In fact, the training, validation, and performance testing are typically conducted with a predetermined set of hyperparameters [89]. These hyperparameters vary widely in type, with some even acting as meta variables, such as the number of hidden layers which is a good illustration for a particular framework. Gaussian Processes (GPs) offer valuable assistance in this optimization process. GPs can efficiently evaluate multiple sets of hyperparameters at a significantly reduced computational cost. Furthermore, GPs can be integrated into Bayesian optimization frameworks to automate the search for optimal hyperparameters [85]. The deep model’s performance relative to its hyperparameters can be conceptualized as a blackbox function with mixed hierarchical variable inputs and therefore heterogeneous data.

Consider a blackbox function  $f : \mathcal{X} \rightarrow \mathbb{R}$ , which outputs a performance score  $f(\mathbf{X}) \in \mathbb{R}$  for a given vector of hyperparameters  $\mathbf{X} \in \mathcal{X}$ . For the MLP problem, the function  $f$  is evaluated by training the deep model knowing the specific set of hyperparameters  $\mathbf{X}$  and then test it to obtain a resulting performance score  $f(\mathbf{X})$ . Therefore, the latter represents the model’s accuracy on a previously unseen data set [8]. While the internal mechanics of  $f$  are understood, the function is treated as an expensive-to-evaluate blackbox problem due to the complexity involved in adjusting billions of model parameters and of fine-tuning them through backpropagation during training [8, 88]. To facilitate the comprehension of our modeling work, Feature Model (FM) has been used to build the tree presented in Figure B.10 that shows how modeling can give insights for a system such as the MLP. First, the selection



of the optimizer determines which hyperparameters are included in the optimization domain. For instance, the decay parameter  $\lambda$  is only considered if the optimizer  $o \in \{\text{Adam}, \text{ASGD}\}$  is ASGD. Second, the optimizer influences the model’s architecture. Specifically, it affects the set of possible values for the number of hidden layers and number of units in each included layer that is represented by a “requires” relationship as it changes the possible bounds. Choices are represented by “alternative” features, as in dropout that is either small or high but not both, whereas the included or not layers are represented by OR features. For the sake of illustration, we have no incompatibilities and therefore, no “excludes” relationship on this problem.

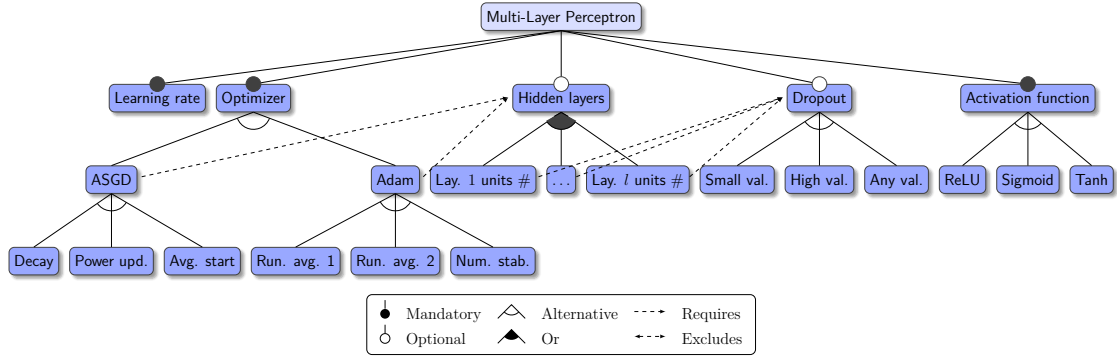


Figure B.10: Feature model for the MLP working example.

The feature model of Figure B.10 presents several limitations. First, continuous variables have non-discrete support that can not be addressed by feature models. However, this remark can partially be addressed by a feature model extension called attribute feature models [1, 147]. Attribute feature models address a key limitation by explicitly encoding dependencies that are otherwise implicit. For example, they capture that including a hidden layer requires specifying both how many units it may contain and which dropout values are valid. They also clarify how the choice of optimizer constraints which architectures are valid, and enable more flexible, partially specified variable definitions by explicitly defining allowable value ranges (supports). Attributes do not necessarily serve as variable supports, and features do not always correspond to optimization or modeling variables. For example, in the Feature Model (FM), “Adam” is considered a feature, whereas in the design space definition, it represents a level of the variable “Optimization.” Similarly, “hidden layers” may be a feature in the FM but not a design variable in the design space. In the design space, the number of hidden layers is treated as a variable, while in the FM, this choice is governed by an “OR” relationship, meaning that determining the number of hidden layers requires counting how many have been selected. These distinctions highlight the need for the hierarchical model introduced in this paper. Unlike traditional feature models and design space graphs, this model is more directly aligned with design variables, making it a complementary approach that bridges the gap between existing representations. With the design space graph approach, the first modeling step is to build the role graph  $G = (N, A)$ , which is presented schematically in Figure B.11. Note that the index  $i$  in  $u_i$  indicates the  $i$ -th hidden layer. For example, if  $l = 3$ , there are three hidden layers, each with its own hyperparameter for the number of units, *i.e.*,  $u_1, u_2, u_3$ . Furthermore, the number of hidden layers  $l \in L_o$  (influenced by the

chosen optimizer) also determines the number of variables associated to the units  $u_i$  in the hidden layers creating a 2-level hierarchy. Also, the sum of the units  $u_i$  affects the allowable dropout rate  $p$ , governed by the inequality

$$\sum_{i=1}^l u_i \leq U^{\text{thr}},$$

where  $U^{\text{thr}} \in \mathbb{N}$  is a predefined threshold. If the inequality is violated, the dropout rate  $p$  is enforced to be at least 0.25, which helps prevent overfitting in large architectures [66]. In addition, motivated by studies suggesting that the Adam optimizer may generalize less effectively than ASGD [121], the dropout rate  $p$  has a broader range, allowing higher values when  $o = \text{Adam}$ .

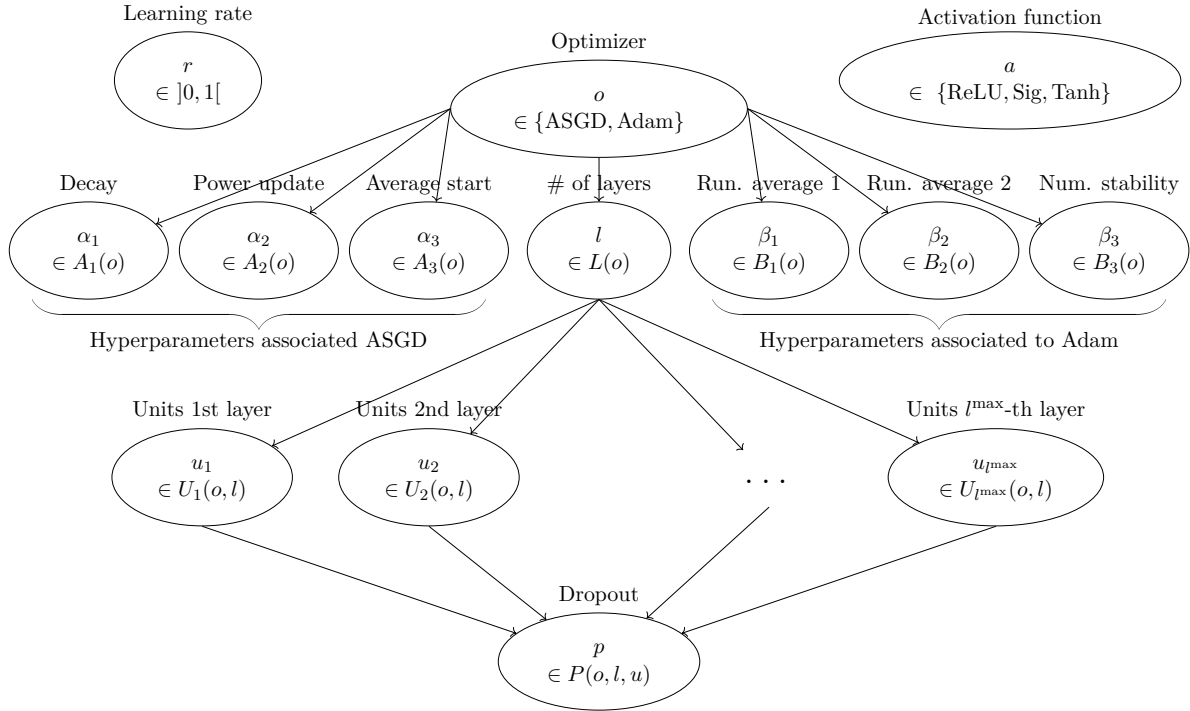


Figure B.11: Role graph  $G$  for the MLP working example.

The role graph  $G$  in Figure B.11 models a great deal of information, including 1) the decree relations, represented by arcs, between the variables, 2) the role of each variable via the position of its corresponding node in the DAG, 3) the depth of each variable, and 4) the dependencies of the belonging sets of meta-decreed and decreed variables with their lower-depth variables. As such, it is more explicit than the feature model. The FM has 5 first-level features, whereas our hierarchical model has 3 roots because the dropout depends on the hidden layers, whose value may be incompatible with the chosen optimizer. Therefore, to solve these incompatibilities, the graph model proposes to choose first the optimizer, then the hidden layer, and then the dropout. The second modeling step is to explicit the component by roles, the role sets and the belonging sets of each meta-decreed and decreed variable in Figure B.11. The meta and neutral roles can be trivially expressed as

$$\mathbf{x}^{\text{m}} = \mathbf{x}_{\text{cat}}^{\text{m}} = o \in \mathcal{X}^{\text{m}} = \{\text{ASGD}, \text{Adam}\},$$

and,

$$\mathbf{x}^{\text{neu}} = (\mathbf{x}_{\text{con}}^{\text{neu}}, \mathbf{x}_{\text{cat}}^{\text{neu}}) = (r, a) \in \mathcal{X}^{\text{neu}} = ]0, 1[ \times \{\text{ReLU}, \text{Sig}, \text{Tanh}\}.$$

For a given optimizer  $\mathbf{x}^{\text{m}} = o \in \{\text{ASGD}, \text{Adam}\}$ , the meta-decreed component and set are expressed as

$$\mathbf{x}^{\text{md}} = (x_{\text{int},1}^{\text{md}}, x_{\text{int},2}^{\text{md}}, \dots, x_{\text{int},l^{\text{max}}+1}^{\text{md}}) = (l, u_1, u_2, \dots, u_{l^{\text{max}}}) = (l, u) \in L(o) \times \prod_{i=1}^{l^{\text{max}}} U_i(l, o)$$

where  $l^{\text{max}} = \max(L_{\text{ASGD}} \cup L_{\text{Adam}})$  is the highest value of number of hidden layers, and

$$L(o) = \begin{cases} L_{\text{ASGD}} & \text{if } o = \text{ASGD}, \\ L_{\text{Adam}} & \text{if } o = \text{Adam}, \end{cases} \quad U_i(o, l) = \begin{cases} U_{\text{ASGD}} & \text{if } o = \text{ASGD} \text{ and } u_i \text{ is included,} \\ U_{\text{Adam}} & \text{if } o = \text{Adam} \text{ and } u_i \text{ is included,} \\ \{\text{EXC}\} & \text{otherwise,} \end{cases}$$

with  $u_i$  is included signifies that  $1 \leq i \leq l$ , *i.e.*, the  $i$ -th hidden layer is included in the architecture of the MLP. In Figure B.11, the number of hidden layers  $l$  is lower-depth than the number of units  $u_i$ , for all  $1 \leq i \leq l^{\text{max}}$ . Hence, the number of hidden layers is placed before the numbers of units  $u_1, u_2, \dots, u_{l^{\text{max}}}$ . To make the example more realistic, further suppose that  $L_{\text{ASGD}} = \{3, 4\}$ ,  $L_{\text{Adam}} = \{3, 4, 5\}$ , and let  $o = \text{ASGD}$  and  $l = 3$ . Hence, the search space can be explicit as

$$\mathbf{x}^{\text{md}} = (x_{\text{int},1}^{\text{md}}, x_{\text{int},2}^{\text{md}}, \dots, x_{\text{int},6}^{\text{md}}) = (l, u_1, u_2, u_3, u_4, u_5) = (l, u) \in \{2, 3, 4\} \times \prod_{i=1}^5 U_i(\text{ASGD}, l),$$

where  $U_i(\text{ASGD}, 3) = U_{\text{ASGD}}$  for  $i \in \{1, 2, 3\}$ , and  $U_j(\text{ASGD}, 3) = \{\text{EXC}\}$  for  $j \in \{4, 5\}$ . For a given optimizer  $o \in \{\text{ASGD}, \text{Adam}\}$ , a given number of hidden layers  $l \in L(o)$  and given numbers of units  $u = (u_1, u_2, \dots, u_5) \in \prod_{i=1}^5 U_i(l, o)$ , the decreed component  $x^{\text{dec}}$  and the decreed set  $\mathcal{X}^{\text{dec}}(x^{\text{m}}, x^{\text{md}})$  are expressed as

$$\mathbf{x}^{\text{dec}} = (x_{\text{con},1}^{\text{dec}}, \dots, x_{\text{con},7}^{\text{dec}}) = (\alpha_1, \alpha_2, \alpha_3, \beta_1, \beta_2, \beta_3, p) \in \prod_{i=1}^3 A_i(o) \times \prod_{j=1}^3 B_j(o) \times P(o, l, u),$$

where,  $\forall i \in \{2, 3\}$  and  $\forall j \in \{1, 2, 3\}$ :

$$A_i(o) = \begin{cases} ]0, 1[ & \text{if } o = \text{ASGD}, \\ \{\text{EXC}\} & \text{if } o = \text{Adam}, \end{cases} \quad A_3(o) = \begin{cases} ]1\text{E}3, 1\text{E}8[ & \text{if } o = \text{ASGD}, \\ \{\text{EXC}\} & \text{if } o = \text{Adam}, \end{cases}$$

$$B_j(o) = \begin{cases} \{\text{EXC}\} & \text{if } o = \text{ASGD}, \\ ]0, 1[ & \text{if } o = \text{Adam}, \end{cases} \quad P(o, l, u) = \begin{cases} [0, 0.5] & \text{if } o = \text{ASGD} \text{ and } \sum_{i=1}^{l^{\text{max}}} u_i \leq U^{\text{thr}}, \\ [0, 0.75] & \text{if } o = \text{Adam} \text{ and } \sum_{i=1}^{l^{\text{max}}} u_i \leq U^{\text{thr}}, \\ [0.25, 0.75] & \text{otherwise.} \end{cases}$$

The hierarchical domain can then be expressed as  $\mathcal{X}_G = \left\{ (x^{\text{m}}, x^{\text{md}}, x^{\text{dec}}, x^{\text{neu}}) : x^{\text{m}} = o \in \right.$

$$\left. \begin{aligned} &\{\text{ASGD}, \text{Adam}\}, x^{\text{md}} = (l, u_1, u_2, \dots, u_5) \in L(o) \times \prod_{i=1}^5 U_i(l, o), x^{\text{dec}} = (\alpha_1, \alpha_2, \alpha_3, \beta_1, \beta_2, \beta_3, p) \in \\ &\prod_{i=1}^3 A_i(o) \times \prod_{j=1}^3 B_j(o) \times P(o, l, u), x^{\text{neu}} = (r, a) \in ]0, 1[ \times \{\text{ReLU}, \text{Sig}, \text{Tanh}\} \end{aligned} \right\}.$$

## Appendix C. SMT Design Space Graph implementation usage

In this section, we present, in Figure C.12, the code that generates the hierarchical design space graph of the Multi-Layer Peceptron hierarchical design space. This design space is adapted for visualization, distance computation and surrogate modeling.

```

# Define the mixed hierarchical design space
design_space = DesignSpaceGraph([
    FloatVariable (0, 1), #Learning rate
    CategoricalVariable ([ "ReLU", "Sigmoid", "Tanh" ]), #3 possible choices
    for the activation function
    CategoricalVariable ([ "ASGD", "Adam" ]), #2 possible choices for the
    optimizer
    FloatVariable (0, 1), #ASGD Decay
    FloatVariable (0, 1), #ASGD Power update
    FloatVariable (0, 1), #ASGD Average start
    FloatVariable (0, 1), #Adam Running Average 1
    FloatVariable (0, 1), #Adam Running Average 2
    FloatVariable (0, 1), #Adam Numerical Stability
    IntegerVariable (1, 3), #for the number of hidden layers (l=x9)
    OrdinalVariable ([ '25', '30', '35', '40', '45' ]), #number of hidden
    neurons layer 1
    OrdinalVariable ([ '25', '30', '35', '40', '45' ]), #number of hidden
    neurons layer 2
    OrdinalVariable ([ '25', '30', '35', '40', '45' ]), #number of hidden
    neurons layer 3
])

#ASGD vs Adam optimizer options activated or deactivated
design_space.declare_decreed_var(decreed_var =3, meta_var =2, meta_value
    =["ASGD"])
design_space.declare_decreed_var(decreed_var =4, meta_var =2, meta_value
    =["ASGD"])
design_space.declare_decreed_var(decreed_var =5, meta_var =2, meta_value
    =["ASGD"])
design_space.declare_decreed_var(decreed_var =6, meta_var =2, meta_value
    =["Adam"])
design_space.declare_decreed_var(decreed_var =7, meta_var =2, meta_value
    =["Adam"])
design_space.declare_decreed_var(decreed_var =8, meta_var =2, meta_value
    =["Adam"])

# Number of hidden layers: Activate x11 when x9 in [2, 3] and x12 when x9
    == 3
design_space.add_value_constraint(var1=9, value1=3, var2=2, value2=["Adam"
    ]) # Forbid 3 hidden layers with Adam
design_space.declare_decreed_var(decreed_var =10, meta_var =9, meta_value
    =[1,2,3])
design_space.declare_decreed_var(decreed_var =11, meta_var =9, meta_value
    =[2,3])
design_space.declare_decreed_var(decreed_var =12, meta_var =9, meta_value
    =3)
design_space.add_value_constraint(var1=10, value1=[ '40', '45' ], var2=2,
    value2=["ASGD"]) # Forbid more than 35 neurons with ASGD
design_space.add_value_constraint(var1=11, value1=[ '40', '45' ], var2=2,
    value2=["ASGD"]) # Forbid more than 35 neurons with ASGD
design_space.add_value_constraint(var1=12, value1=[ '40', '45' ], var2=2,
    value2=["ASGD"]) # Forbid more than 35 neurons with ASGD

```

Figure C.12: AdsgDesignSpaceImpl definition for the neural network problem.

## Appendix D. Symmetric Positive Definiteness of hierachical kernels

In this section, we show that our proposed hierarchical kernel—built from neutral, meta-level, and decreed-variable components—yields a symmetric positive-definite covariance function suitable for Gaussian-process models on arbitrarily nested, mixed-type variable spaces. The new kernel  $k$  that we propose for hierarchical variables extends a previous work [135] and is given by

$$k(\mathbf{X}, \mathbf{X}') = k_{\text{neu}}(\mathbf{X}_{\text{neu}}, \mathbf{X}'_{\text{neu}}) \times k_{\text{m}}(\mathbf{X}_{\text{m}}, \mathbf{X}'_{\text{m}}) \times k_{\text{m,dec}}([\mathbf{X}_{\text{m}}, \mathbf{X}_{\text{inc}}(\mathbf{X}_{\text{m}})], [\mathbf{X}'_{\text{m}}, \mathbf{X}'_{\text{inc}}(\mathbf{X}'_{\text{m}})]),$$

where  $k_{\text{neu}}$ ,  $k_{\text{m}}$  and  $k_{\text{m,dec}}$  are as follows:

- $k_{\text{neu}}$  represents the neutral kernel that encompasses both categorical and quantitative neutral variables, *i.e.*,  $k_{\text{neu}}$  can be decomposed into two parts  $k_{\text{neu}}(\mathbf{X}_{\text{neu}}, \mathbf{X}'_{\text{neu}}) = k^{\text{cat}}(\mathbf{X}_{\text{neu}}^{\text{cat}}, \mathbf{X}'_{\text{neu}}^{\text{cat}}) \times k^{\text{qnt}}(\mathbf{X}_{\text{neu}}^{\text{qnt}}, \mathbf{X}'_{\text{neu}}^{\text{qnt}})$ . The categorical kernel, denoted  $k^{\text{cat}}$ , could be any Symmetric Positive Definite (SPD) [132] mixed kernel. For the quantitative (integer or continuous) variables, a distance-based kernel is used. The chosen quantitative kernel (e.g., exponential or Matérn), always depends on a given distance  $d$ . For example, the  $n$ -dimensional exponential kernel gives

$$k^{\text{qnt}}(\mathbf{X}^{\text{qnt}}, \mathbf{X}'^{\text{qnt}}) = \prod_{i=1}^n \exp(-d(\mathbf{X}_i^{\text{qnt}}, \mathbf{X}'_i^{\text{qnt}})).$$

- $k_{\text{m}}$  is the meta variables related kernel. It is also separated into two parts:  $k_{\text{m}}(\mathbf{X}_{\text{m}}, \mathbf{X}'_{\text{m}}) = k^{\text{cat}}(\mathbf{X}_{\text{m}}^{\text{cat}}, \mathbf{X}'_{\text{m}}^{\text{cat}})k^{\text{qnt}}(\mathbf{X}_{\text{m}}^{\text{qnt}}, \mathbf{X}'_{\text{m}}^{\text{qnt}})$  where the quantitative kernel is ordered and not continuous because meta variables take value in a finite set.
- $k_{\text{m,dec}}$  is an SPD kernel that models the correlations between the meta levels (all the possible subspaces) and the decreed variables. It is a quantitative kernel depending on the aforementioned graph-structure distance  $\overline{\text{dist}}$ . In particular, we have developed several continuous relaxation to make any distance, such as the new graph-structure one, to induce a categorical kernel. This allows to generalize here the previous kernel [130] to also handle decreed categorical variables as described in [32].

**Theorem 1.** *The kernel  $K^{\text{naive}}$  defined as follows is not a SPD kernel.*

$$\begin{cases} K^{\text{naive}}(\mathbf{X}, \mathbf{X}') = k_{\text{dec}}(\mathbf{X}_{\text{inc}}(\mathbf{X}'_{\text{m}}), \mathbf{X}'_{\text{inc}}(\mathbf{X}'_{\text{m}}))k_{\text{neu}}(\mathbf{X}_{\text{neu}}, \mathbf{X}'_{\text{neu}}), & \text{if } \mathbf{X}_{\text{m}} = \mathbf{X}'_{\text{m}} \\ K^{\text{naive}}(\mathbf{X}, \mathbf{X}') = k_{\text{m}}(\mathbf{X}_{\text{m}}, \mathbf{X}'_{\text{m}})k_{\text{neu}}(\mathbf{X}_{\text{neu}}, \mathbf{X}'_{\text{neu}}), & \text{if } \mathbf{X}_{\text{m}} \neq \mathbf{X}'_{\text{m}} \end{cases} \quad (\text{D.1})$$

*Proof.*  $K^{\text{naive}}$  is a kernel if and only if  $K^{\text{naive}}$  can be written as  $K^{\text{naive}}(\mathbf{X}, \mathbf{X}') = \kappa(d(\mathbf{X}, \mathbf{X}'))$  with  $\kappa$  being an SPD function and  $d$  being a distance in a given Hilbert space. If the two continuous decreed inputs  $\mathbf{X}_{\text{dec}}$  and  $\mathbf{X}'_{\text{dec}}$  are in the same subspace ( $\mathbf{X}_{\text{m}} = \mathbf{X}'_{\text{m}}$ ), then  $k_{\text{m}}(\mathbf{X}_{\text{m}}, \mathbf{X}_{\text{m}}) = 1$  and  $K^{\text{naive}}(\mathbf{X}, \mathbf{X}') = k_{\text{dec}}(\mathbf{X}_{\text{inc}}(\mathbf{X}_{\text{m}}), \mathbf{X}'_{\text{inc}}(\mathbf{X}'_{\text{m}}))$ . This works without any problem, a categorical variable being fully correlated with itself.

On the contrary, if the two continuous inputs  $\mathbf{X}_{\text{dec}}$  and  $\mathbf{X}'_{\text{dec}}$  lie in two different subspaces ( $\mathbf{X}_{\text{m}} \neq \mathbf{X}'_{\text{m}}$ ), then, we have  $k_{\text{dec}}(\mathbf{X}_{\text{dec}}, \mathbf{X}'_{\text{dec}}) = 1 \implies d(\mathbf{X}_{\text{inc}}(\mathbf{X}_{\text{m}}), \mathbf{X}'_{\text{inc}}(\mathbf{X}'_{\text{m}})) = 0$ .

We know that a distance is defined such that  $d(\mathbf{X}, \mathbf{X}') = 0 \Leftrightarrow \mathbf{X} = \mathbf{X}'$  (Identity of indiscernibles). Yet, we have  $d(\mathbf{X}_{\text{inc}}(\mathbf{X}_{\text{m}}), \mathbf{X}'_{\text{inc}}(\mathbf{X}'_{\text{m}})) = 0$  and  $\mathbf{X}_{\text{inc}}(\mathbf{X}_{\text{m}}) \neq \mathbf{X}'_{\text{inc}}(\mathbf{X}'_{\text{m}})$ .  $d$  is not a distance because it is always equal to 0 for points in distinct decreed spaces. Therefore the kernel vanishes to 1 and the correlation matrix is degenerated and can not be SPD.

Based on this proof, the idea of the arc-kernel is to have a constant residual distance between distinct subspaces. In other words, there is a non-zero distance between  $\mathcal{X}(\mathbf{X}_{\text{m}})$  and  $\mathcal{X}(\mathbf{X}'_{\text{m}})$  if  $\mathbf{X}_{\text{m}} \neq \mathbf{X}'_{\text{m}}$ . □

**Theorem 2.** *Our Alg-Kernel kernel is SPD and so is  $k$  defined in Eq. (D.1).*

*Proof.* Let  $I_{\mathbf{X}}$  be the subset of indices  $i \in I_{\text{dec}}$  that are decreed-included by  $\mathbf{X}_{\text{m}}$  such that  $I_{\mathbf{X}, \mathbf{X}'}^{\text{inter}} = I_{\mathbf{X}} \cap I_{\mathbf{X}'}$ . Let  $d_E([x_{\mathbf{X}}, x_{\mathbf{X}'}], [y_{\mathbf{X}}, y_{\mathbf{X}'}]) = \theta_i \sqrt{(x_{\mathbf{X}} - x_{\mathbf{X}'})^2 + (y_{\mathbf{X}} - y_{\mathbf{X}'})^2}$  be an Euclidean distance in  $\mathbb{R}^2 \times \mathbb{R}^2$ . Due to [75, Proposition 2], we only need to show that, for any

two inputs  $\mathbf{X}, \mathbf{X}' \in \mathcal{X}$ , the isometry condition  $d_E(f_i^{alg}(\mathbf{X}), f_i^{alg}(\mathbf{X}'))$  holds for a given function  $f_i^{alg}$ , that is equivalent to having a Hilbertian metric. In other words,  $d_E$  is isomorphic to an  $L^2$  norm [70]. Such kernels are well-known and referred as “substitution kernels with euclidean distance” [145].

$\forall i \in I_{dec}, f_i^{alg}(\mathbf{X}_{dec})$  is defined by

$$\begin{cases} f_i^{alg}(\mathbf{X}_{inc}) = [\frac{1 - ((\mathbf{X}_{dec})_i)^2}{1 + ((\mathbf{X}_{dec})_i)^2}, \frac{2(\mathbf{X}_{dec})_i}{1 + ((\mathbf{X}_{dec})_i)^2}] & \text{if } i \in I_u \\ f_i^{alg}(\mathbf{X}_{dec}) = [0, 0] & \text{otherwise} \end{cases} \quad (\text{D.2})$$

Case 1:  $i \in I_{dec}, i \notin I_{\mathbf{X}}, i \notin I_{\mathbf{X}'}$ .

$$d_E(f_i^{alg}(\overline{\mathbf{X}}_{dec}), f_i^{alg}(\overline{\mathbf{X}'}_{dec})) = d_E([0, 0], [0, 0]) = 0.$$

Therefore, the complementary space is not relevant, as for the arc-kernel.

Case 2:  $i \in I_{dec}, i \in I_{\mathbf{X}}, i \notin I_{\mathbf{X}'}$ .

$$\begin{aligned} d_E(f_i^{alg}(\mathbf{X}_{dec}), f_i^{alg}(\overline{\mathbf{X}'}_{dec})) &= d_E([\frac{1 - ((\mathbf{X}_{dec})_i)^2}{1 + ((\mathbf{X}_{dec})_i)^2}, \frac{2(\mathbf{X}_{dec})_i}{1 + ((\mathbf{X}_{dec})_i)^2}], [0, 0]) \\ &= \theta_i. \end{aligned}$$

This case corresponds to the kernel  $K_m^{alg}(\mathbf{X}_m, \mathbf{X}'_m)$  when  $\mathbf{X}_m \neq \mathbf{X}'_m$ .

Case 3:  $i \in I_{dec}, i \in I_{\mathbf{X}, \mathbf{X}'}^{inter}$ .

$$\begin{aligned} & d_E(f_i^{alg}(\mathbf{X}_{dec}), f_i^{alg}(\mathbf{X}'_{dec})) \\ &= d_E\left(\left[\frac{1 - ((\mathbf{X}_{dec})_i)^2}{1 + ((\mathbf{X}_{dec})_i)^2}, \frac{2(\mathbf{X}_{dec})_i}{1 + ((\mathbf{X}_{dec})_i)^2}\right], \left[\frac{1 - ((\mathbf{X}'_{dec})_i)^2}{1 + ((\mathbf{X}'_{dec})_i)^2}, \frac{2(\mathbf{X}'_{dec})_i}{1 + ((\mathbf{X}'_{dec})_i)^2}\right]\right) \\ &= 2\theta_i \frac{|(\mathbf{X}_{dec})_i - (\mathbf{X}'_{dec})_i|}{\sqrt{((\mathbf{X}_{dec})_i)^2 + 1} \sqrt{((\mathbf{X}'_{dec})_i)^2 + 1}} \end{aligned}$$

This case corresponds to the kernel  $K_{dec}^{alg}(\mathbf{X}_{dec}(\mathbf{X}_m), \mathbf{X}'_{dec}(\mathbf{X}'_m))$  when  $\mathbf{X}_m = \mathbf{X}'_m$ .

Therefore, there exists an isometry between our algebraic distance and the euclidean distance. The distance being well-defined for any given kernel, the matrix obtained with our model is SPD.

Although, in [75], they also do the demonstration of the metric property of their distance formally. The non-negativity and symmetry of  $d^{alg}$  are trivially proven knowing that the hyperparameters  $\theta$  are strictly positive. To prove the triangle inequality, consider  $(u, v, w) \in \mathcal{X}^3$ .

Case 1:  $i \in I_{dec}, i \notin I_u, i \notin I_v$ .

$$d^{alg}(u_i, v_i) = 0 \leq d^{alg}(u_i, w_i) + d^{alg}(w_i, v_i) \text{ by non negativity.}$$

Case 2:  $i \in I_{dec}, i \in I_u, i \notin I_v$ .

$$\bullet \quad i \in I_w, \quad d^{alg}(u_i, v_i) = \theta_i \leq d^{alg}(u_i, w_i) + \theta_i \text{ by non negativity.}$$



- $i \notin I_w$ ,  $d^{\text{alg}}(u_i, v_i) = \theta_i \leq \theta_i + d^{\text{alg}}(w_i, v_i)$  by non negativity.

Case 3:  $i \in I_{\text{dec}}, i \in I_{u,v}^{\text{inter}}$ .

- $i \notin I_w$ ,  $d^{\text{alg}}(u_i, v_i) = 2\theta_i \frac{|u_i - v_i|}{\sqrt{(u_i)^2 + 1} \sqrt{(v_i)^2 + 1}} \leq \theta_i + \theta_i$  for  $(u_i, v_i) \in [0, 1]^2$ .
- $i \in I_w$ , Knowing that  $\frac{|a-c|}{\sqrt{a^2+1}\sqrt{c^2+1}} + \frac{|c-b|}{\sqrt{c^2+1}\sqrt{b^2+1}} \geq \frac{|a-b|}{\sqrt{a^2+1}\sqrt{b^2+1}}$ , we have  $d^{\text{alg}}(u_i, v_i) = 2\theta_i \frac{|u_i - v_i|}{\sqrt{(u_i)^2 + 1} \sqrt{(v_i)^2 + 1}} \leq d^{\text{alg}}(u_i, w_i) + d^{\text{alg}}(w_i, v_i)$ .

Using [72, Theorem 3], any graph-structure distance is well-defined if and only if  $\sup\{d(\mu, \nu) : \mu, \nu \in \mathcal{X}^2\}/2 \leq \theta_i$ . This can make the proof easier and faster as follows. First, we can compute the maximum of the algebraic distances which gives  $\max_{(x,y) \in \mathbb{R}^2} d^{\text{alg}}(x, y) = \max_{(x,y) \in \mathbb{R}^2} 2\theta_i |x - y| \sqrt{\frac{1}{x^2+1}} \sqrt{\frac{1}{y^2+1}} = d^{\text{alg}}(x, -\frac{1}{x}) = 2\theta_i$ . Then, we just have to check that  $2\theta_i/2 \leq \theta_i$  which is the case. This theorem brings two interesting insights on our distance, first it is a limit case as the distance between two non-interacting subspaces is properly maximized and second, the algebraic circle based distance is well-constructed as the maximal distance correspond to the maximal arc of 1 radian making it a generalization of the Arc-distance [159].

□

## References

- [1] A. Abbas and I. F. Siddiqui and S. U. Lee. Multi-objective optimization of feature model in software product line: Perspectives and challenges. *Indian Journal of Science and Technology*, 2016.
- [2] M.A. Abramson. Mixed Variable Optimization of a Load-Bearing Thermal Insulation System Using a Filter Pattern Search Algorithm. *Optimization and Engineering*, 5(2):157–177, 2004.
- [3] R. Agrawal, C. Faloutsos, and A. Swami. Efficient similarity search in sequence databases. In *Foundations of Data Organization and Algorithms, FODO'93*, 1993.
- [4] A. Aleti., B. Buhnova, L. Grunske, A. Koziolk, and I. Meedeniya. Software Architecture Optimization Methods: A Systematic Literature Review. *IEEE Transactions on Software Engineering*, 39(5):658–683, 2013.
- [5] E. De Angelis, F. Fioravanti, J. Gallagher, M. Hermenegildo, A. Pettorossi, and M. Proietti. Analysis and transformation of constrained horn clauses for program verification. *Theory and Practice of Logic Programming*, 22:974–1042, 2022.
- [6] R. Angles and C. Gutierrez. *Graph Data Management: Fundamental Issues and Recent Developments*. Springer Series in Data-Centric Systems and Applications, 2018.
- [7] M. Asadi, G. Gröner, B. Mohabbati, and D. Gašević. Goal-oriented modeling and verification of feature-oriented product lines. *Software & Systems Modeling*, 15:257–279, 2016.
- [8] C. Audet, E. Hallé-Hannan, and S. Le Digabel. A general mathematical framework for constrained mixed-variable blackbox optimization problems with meta and categorical variables. *Operations Research Forum*, 4:1–37, 2023.

- [9] C. Audet and W. Hare. *Derivative-Free and Blackbox Optimization*. Springer Series in Operations Research and Financial Engineering, 2017.
- [10] F. Baader, D. Calvanese, D. McGuinness, D. Nardi, and P. Patel-Schneider. *The Description Logic Handbook: Theory, Implementation, and Applications*. Cambridge University Press, 2007.
- [11] P. Balança and E. Herbin. A set-indexed ornstein-uhlenbeck process. *Electron. Commun. Probab.*, 17:1–14, 2012.
- [12] J. Bang-Jensen and M. Kriesell. Disjoint directed and undirected paths and cycles in digraphs. *Theoretical Computer Science*, 410:5138–5144, 2009.
- [13] L. Baraton, A. Urbano, L. Brevault, and M. Balesdent. Comparative review of multi-disciplinary design analysis and optimization architectures for the preliminary design of a liquid rocket engine. In *Aerospace Europe Conference 2023*, 2023.
- [14] N. Bartoli, T. Lefebvre, S. Dubreuil, R. Olivanti, R. Priem, N. Bons, J.R.R.A Martin, and J. Morlier. Adaptive modeling strategy for constrained global optimization with application to aerodynamic wing design. *Aerospace Science and Technology*, 90:85–102, 2019.
- [15] N. Bartoli, T. Lefebvre, R. Lafage, P. Saves, Y. Diouane, J. Morlier, J. H. Bussemaker, G. Donelli, J. M. Gomes de Mello, M. Mandorino, and P. Della Vecchia. Multi-objective Bayesian optimization with mixed-categorical design variables for expensive-to-evaluate aeronautical applications. In *AeroBest 2023*, 2023.
- [16] Don Batory. Feature models, grammars, and propositional formulas. In *International Conference on Software Product Lines*, pages 7–20. Springer, 2005.
- [17] David Benavides, Sergio Segura, and Antonio Ruiz-Cortés. Automated analysis of feature models 20 years later: A literature review. *Information systems*, 35(6):615–636, 2010.
- [18] M. Bender, M. Farach-Colton, G. Pemmasani, S. Skiena, and P. Sumazin. Lowest common ancestors in trees and directed acyclic graphs. *Journal of Algorithms*, 57:75–94, 2005.
- [19] A. Bhosekar and M. Ierapetritou. Advances in surrogate based modeling, feasibility analysis, and optimization: A review. *Computers & Chemical Engineering*, 108:250–267, 2018.
- [20] D. Bihanic and T. Polacsek. Models for visualisation of complex information systems. In *16th International Conference on Information Visualisation*, 2012.
- [21] D. Blumenthal and J. Gamper. On the exact computation of the graph edit distance. *Pattern Recognition Letters*, 134:46–57, 2020.
- [22] M. A. Bouhlel, N. Bartoli, R.G. Regis, A. Otsmane, and J. Morlier. Efficient global optimization for high-dimensional constrained problems by using the Kriging models combined with the partial least squares method. *Engineering Optimization*, 50:2038–2053, 2018.
- [23] M. A. Bouhlel, J. T. Hwang, N. Bartoli, R. Lafage, J. Morlier, and J. R. R. A. Martins. A Python surrogate modeling framework with derivatives. *Advances in Engineering Software*, 135:102662, 2019.

- [24] T. Bourdais, P. Batlle, X. Yang, R. Baptista, N. Rouquette, and H. Owhadi. Codiscovering graphical structure and functional relationships within data: A gaussian process framework for connecting the dots. *Proceedings of the National Academy of Sciences*, 121(32):e2403449121, 2024.
- [25] A. Bravais. Analyse mathématique sur les probabilités des erreurs de situation d’un point. *Mémoires de l’Académie royale des sciences de l’Institut imperial de France*, 1844.
- [26] J-M. Bruel, B. Combemale, E. Guerra, J-M. Jézéquel, J. Kienzle, J. De Lara, G. Mussbacher, E. Syriani, and H. Vangheluwe. Comparing and classifying model transformation reuse approaches across metamodels. *Software and Systems Modeling*, 19:441–465, 2020.
- [27] H. Busemann. The isoperimetric problem in the minkowski plane. *American Journal of Mathematics*, 69:863–871, 1947.
- [28] J. Buss and J. Goldsmith. Nondeterminism within  $P^*$ . *SIAM Journal on Computing*, 22:560–572, 1993.
- [29] J. H. Bussemaker. SBArchOpt: Surrogate-based architecture optimization. *Journal of Open Source Software*, 8:5564, 2023.
- [30] J. H. Bussemaker, L. Boggero, and P. D. Ciampa. From system architecting to system design and optimization: A link between MBSE and MDAO. In *INCOSE International Symposium*, 2022.
- [31] J. H. Bussemaker, L. Boggero, and B. Nagel. System architecture design space exploration: Integration with computational environments and efficient optimization. In *AIAA AVIATION 2024 FORUM*, 2024.
- [32] J. H. Bussemaker, P. Saves, N. Bartoli, T. Lefebvre, and R. Lafage. System architecture optimization strategies: Dealing with expensive hierarchical problems. *Journal of Global Optimization*, 90:1–45, 2024.
- [33] J. H. Bussemaker, T. De Smedt, G. La Rocca, P. D. Ciampa, and B. Nagel. System architecture optimization: An open source multidisciplinary aircraft jet engine architecting problem. In *AIAA AVIATION 2021 Forum*, page 3078, 2021.
- [34] J.H. Bussemaker, P.D. Ciampa, T. De Smedet, B. Nagel, and G. La Rocca. System Architecture Optimization: An Open Source Multidisciplinary Aircraft Jet Engine Architecting Problem. In *AIAA AVIATION 2021 Forum*, AIAA AVIATION Forum. American Institute of Aeronautics and Astronautics, 2021.
- [35] J.H. Bussemaker, P.D. Ciampa, and B. Nagel. System architecture design space exploration: An approach to modeling and optimization. In *AIAA AVIATION 2020 Forum*, AIAA AVIATION Forum. American Institute of Aeronautics and Astronautics, 2020.
- [36] D. Butturi-Gomes and M. Petrere. Edge influence and population aggregation: On point and interval statistical performances of morisita patchiness index estimators in different sampling schemes. *Ecological Indicators*, 108:105736, 2020.
- [37] R. Carpintero Perez, S. Da Veiga, J. Garnier, and B. Staber. Gaussian process regression with sliced wasserstein weisfeiler-lehman graph kernels. In *International Conference on Artificial Intelligence and Statistics*, 2024.
- [38] E. Cazelles, A. Robert, and F. Tobar. The wasserstein-fourier distance for stationary

- time series. *IEEE Transactions on Signal Processing*, 69:709–721, 2020.
- [39] P-A. Champin and C. Solnon. Measuring the similarity of labeled graphs. In *Case-Based Reasoning Research and Development: 5th International Conference on Case-Based Reasoning*, 2003.
  - [40] A. Chan, A. Pires, T. Polacsek, S. Roussel, F. Bouissière, C. Cuiller, and P-E Dereux. Goal modelling: Design and manufacturing in aeronautics. In *International Conference on Research Challenges in Information Science*, 2023.
  - [41] A. Chan, A. Fernandes Pires, and T. Polacsek. Trying to elicit and assign goals to the right actors. In *Conceptual Modeling: 41st International Conference, ER 2022*, 2022.
  - [42] G. Chartrand, G. Kubicki, and M. Schultz. Graph similarity and distance in graphs. *Aequationes Mathematicae*, 55:129–145, 1998.
  - [43] J. Chen, Y. Ng, L. Lin, X. Zhang, and S. Li. On triangle inequalities of correlation-based distances for gene expression profiles. *BMC bioinformatics*, 24:40, 2023.
  - [44] X. Chen, C. Ge, M. Wang, and J. Wang. Supervised contrastive few-shot learning for high-frequency time series. In *Proceedings of the 37th AAAI Conference on Artificial Intelligence (AAAI 2023)*, 2023.
  - [45] H. Cho, Y. Kim, E. Lee, D. Choi, Y. Lee, and W. Rhee. Basic enhancement strategies when using Bayesian optimization for hyperparameter tuning of deep neural networks. *IEEE access*, 8:52588–52608, 2020.
  - [46] R. Cilibrasi and P. Vitányi. Clustering by compression. *IEEE Transactions on Information theory*, 51:1523–1545, 2005.
  - [47] G. Coenders and W. Saris. Categorization and measurement quality. the choice between pearson and polychoric correlations. *The Multitrait-Multimethod approach to evaluate measurement instruments*, pages 125–144, 1995.
  - [48] E. Crawley, B. Cameron, and D. Selva. *System architecture: strategy and product development for complex systems*. Prentice Hall Press, 2015.
  - [49] S. Da Veiga. Global sensitivity analysis with dependence measures. *Journal of Statistical Computation and Simulation*, 85:1283–1305, 2015.
  - [50] C. David, S. Delbecq, S. Defoort, P. Schmollgruber, E. Benard, and V. Pommier-Budinger. From FAST to FAST-OAD: An open source framework for rapid overall aircraft design. *IOP Conference Series: Materials Science and Engineering*, 1024:012062, 2021.
  - [51] K. Deb, A. Pratap, S. Agarwal, and T. Meyarivan. A fast and elitist multiobjective genetic algorithm: NSGA-II. *IEEE Transactions on Evolutionary Computation*, 6(2):182–197, 2002.
  - [52] M. Deza and E. Deza. Other distances. *Encyclopedia of Distances*, 1:661–699, 2014.
  - [53] J. Ellson, E. Gansner, L. Koutsofios, S. North, and G. Woodhull. Graphviz—open source graph drawing tools. In *Graph Drawing: 9th International Symposium, GD 2001 Vienna, Austria, September 23–26, 2001 Revised Papers 9*, 2002.
  - [54] P. Esser, M. Fleissner, and D. Ghoshdastidar. Non-parametric representation learning with kernels. In *Proceedings of the AAAI Conference on Artificial Intelligence*, 2024.
  - [55] N. Fellmann, C. Blanchet-Scalliet, C. Helbert, A. Spagnol, and D. Sinoquet. Kernel-

- based sensitivity analysis for (excursion) sets. *Technometrics*, 67:1–13, 2024.
- [56] A. Feragen, F. Lauze, and S. Hauberg. Geodesic exponential kernels: When curvature and linearity conflict. In *Proceedings of the IEEE conference on computer vision and pattern recognition*, pages 3032–3042, 2015.
  - [57] M. Fernández and G. Valiente. A graph distance metric combining maximum common subgraph and minimum common supergraph. *Pattern Recognition Letters*, 22:753–758, 2001.
  - [58] M. E. A. Fouda, E. J. Adler, J. H. Bussemaker, J. R. R. A. Martins, D. F. Kurtulus, L. Boggero, and B. Nagel. Automated hybrid propulsion model construction for conceptual aircraft design and optimization. In *33rd Congress of the International Council of the Aeronautical Sciences, ICAS 2022*, 2022.
  - [59] P. I. Frazier. A Tutorial on Bayesian Optimization. *ArXiv preprint*, 2018.
  - [60] L. Friedli, A. Gautier, A. Broccard, and D. Ginsbourger. Crps-based targeted sequential design with application in chemical space. *arXiv preprint arXiv:2503.11250*, 2025.
  - [61] A. Sanfeliu K. Fu. A distance measure between attributed relational graphs for pattern recognition. *IEEE transactions on systems, man, and cybernetics*, 3:353–362, 1983.
  - [62] X. Gao, B. Xiao, D. Tao, and X. Li. A survey of graph edit distance. *Pattern Analysis and applications*, 13:113–129, 2010.
  - [63] A. Gardner, C.A. Duncan, J. Kanno, and R.R. Selmic. On the Definiteness of Earth Mover’s Distance and Its Relation to Set Intersection. *IEEE Transaction on Cybernetics*, 48(11):3184–3196, 2018.
  - [64] R. Gómez-Bombarelli, J. Wei, D. Duvenaud, J. Hernández-Lobato, B. Sánchez-Lengeling, D. Sheberla, J. Aguilera-Iparraguirre, T. Hirzel, R. Adams, and A. Aspuru-Guzik. Automatic chemical design using a data-driven continuous representation of molecules. *ACS central science*, 4:268–276, 2018.
  - [65] F. Gonzalez-Lopez, L. Pufahl, J. Munoz-Gama, V. Herskovic, and M. Sepúlveda. Case model landscapes: toward an improved representation of knowledge-intensive processes using the fcm-language. *Software and Systems Modeling*, 20:1353–1377, 2021.
  - [66] I. Goodfellow, Y. Bengio, and A. Courville. *Deep Learning*. MIT Press, 2016.
  - [67] A. Goshtasby. Similarity and dissimilarity measures. *Image registration: Principles, tools and methods*, 1:7–66, 2012.
  - [68] M. Grohe and P. Schweitzer. The graph isomorphism problem. *Communications of the ACM*, 63:128–134, 2020.
  - [69] R. Grosse, R. Salakhutdinov, W. Freemab, and J. Tenenbaum. Exploiting compositionality to explore a large space of model structures. In *Uncertainty in AI (UAI)*, 2012.
  - [70] B. Haasdonk and C. Bahlmann. Learning with distance substitution kernels. *Joint pattern recognition symposium*, 3175:220–227, 2004.
  - [71] E. Hallé-Hannan. Cadre mathématique pour l’optimisation de boîtes noires avec variables métag et catégorielles. Master’s thesis, Polytechnique Montréal, 2022. Available at <https://publications.polymtl.ca/10286/>.

- [72] E. Hallé-Hannan, C. Audet, Y. Diouane, S. Le Digabel, and P. Saves. A distance for mixed-variable and hierarchical domains with meta variables. *ArXiv preprint*, 2025.
- [73] M. Halstrup. *Black-Box Optimization of Mixed Discrete-Continuous Optimization Problems*. PhD thesis, TU Dortmund, 2016.
- [74] Y. Hung, V.R. Joseph, and S.N. Melkote. Design and Analysis of Computer Experiments With Branching and Nested Factors. *Technometrics*, 51(4):354–365, 2009.
- [75] F. Hutter and M. A. Osborne. A kernel for hierarchical parameter spaces. *ArXiv preprint*, 2013.
- [76] F. Hutter and M.A. Osborne. A Kernel for Hierarchical Parameter Spaces. Technical Report 1310.5738, ArXiv, 2013.
- [77] H. Jiang, Y. Shen, Y. Li, W. Zhang, C. Zhang, and B. Cui. Openbox: A Python toolkit for generalized black-box optimization. *ArXiv preprint*, 2023.
- [78] J. Jiang and D. Conrath. Semantic similarity based on corpus statistics and lexical taxonomy. *ArXiv preprint*, 1997.
- [79] D. R. Jones. A taxonomy of global optimization methods based on response surfaces. *Journal of Global Optimization*, 21:345–383, 2001.
- [80] K. Kaneiwa. Order-sorted logic programming with predicate hierarchy. *Artificial Intelligence*, 158:155–188, 2004.
- [81] R. Karlsson, L. Bliet, S. Verwer, and M. de Weerd. Continuous surrogate-based optimization algorithms are well-suited for expensive discrete problems. In *Artificial Intelligence and Machine Learning*, 2021.
- [82] T. Karunaratne and H. Boström. Graph propositionalization for random forests. In *2009 International Conference on Machine Learning and Applications*, 2009.
- [83] M. Kejriwal. Knowledge graphs: A practical review of the research landscape. *Information*, 13:161–178, 2022.
- [84] E. Keogh and S. Kasetty. On the need for time series data mining benchmarks: a survey and empirical demonstration. In *Proceedings of the eighth ACM SIGKDD international conference on Knowledge discovery and data mining*, 2002.
- [85] A. Klein, S. Falkner, S. Bartels, P. Hennig, and F. Hutter. Fast Bayesian Optimization of Machine Learning Hyperparameters on Large Datasets. Technical Report 1605.07079, arXiv, 2017.
- [86] M. Kokkolaras, C. Audet, and J.E. Dennis, Jr. Mixed variable optimization of the Number and composition of heat intercepts in a thermal insulation system. *Optimization and Engineering*, 2(1):5–29, 2001.
- [87] V. Kvasnička, J. Pospíchal, and V. Baláž. Reaction and chemical distances and reaction graphs. *Theoretica chimica acta*, 79:65–79, 1991.
- [88] D. Lakhamiri. HyperNOMAD. <https://github.com/bbopt/HyperNOMAD>, 2019.
- [89] D. Lakhamiri, S. Le Digabel, and C. Tribes. HyperNOMAD: Hyperparameter Optimization of Deep Neural Networks Using Mesh Adaptive Direct Search. *ACM Transactions on Mathematical Software*, 47(3), 2021.
- [90] R. Le Riche and V. Picheny. Revisiting Bayesian optimization in the light of the coco benchmark. *Structural and Multidisciplinary Optimization*, 64:3063–3087, 2021.

- [91] M. Lindauer, K. Eggensperger, M. Feurer, A. Biedenkapp, D. Deng, C. Benjamins, T. Ruhkopf, R. Sass, and F. Hutter. BOAH: A tool suite for multi-fidelity Bayesian optimization & analysis of hyperparameters. *ArXiv preprint*, 2019.
- [92] M. Lindauer, K. Eggensperger, M. Feurer, A. Biedenkapp, D. Deng, C. Benjamins, T. Ruhkopf, R. Sass, and F. Hutter. SMAC3: A versatile Bayesian optimization package for hyperparameter optimization. *Journal of Machine Learning Research*, 23:1–9, 2022.
- [93] S. Lucidi and V. Piccialli. A Derivative-Based Algorithm for a Particular Class of Mixed Variable Optimization Problems. *Optimization Methods and Software*, 17(3–4):317–387, 2004.
- [94] S. Lucidi, V. Piccialli, and M. Sciandrone. An Algorithm Model for Mixed Variable Programming. *SIAM Journal on Optimization*, 15(4):1057–1084, 2005.
- [95] J. Gibbon M. Kendall. *Rank correlation methods*. Oxford University Press, 1948.
- [96] P-F. Marteau and S. Gibet. On recursive edit distance kernels with application to time series classification. *IEEE transactions on neural networks and learning systems*, 26:1121–1133, 2014.
- [97] J.R.R.A. Martins and A. Ning. *Engineering Design Optimization*. Cambridge University Press, 2022.
- [98] D. Mavris, C. de Tenorio, and M. Armstrong. Methodology for aircraft system architecture definition. In *46th AIAA Aerospace Sciences Meeting and Exhibit*, 2008.
- [99] M. Minsky. A framework for representing knowledge. *Artificial Intelligence*, 306:1–81, 1974.
- [100] T. Mitchell, R. Keller, and S.Kedar-Cabelli. Explanation-based generalization: A unifying view. *Machine learning*, 1:47–80, 1986.
- [101] M. Neuhaus and H. Bunke. Self-organizing maps for learning the edit costs in graph matching. *IEEE Transactions on Systems, Man, and Cybernetics, Part B (Cybernetics)*, 35:503–514, 2005.
- [102] M. Neuhaus and H. Bunke. A convolution edit kernel for error-tolerant graph matching. In *18th International Conference on Pattern Recognition (ICPR’06)*, volume 4, pages 220–223, 2006.
- [103] G. Nikolentzos, G. Siglidis, and M. Vazirgiannis. Graph kernels: A survey. *Journal of Artificial Intelligence Research*, 72:943–1027, 2021.
- [104] S. Nishimura and T. Hiramatsu. A generalization of the lee distance and error correcting codes. *Discrete applied mathematics*, 156:588–595, 2008.
- [105] J. Novak. Concept mapping: A useful tool for science education. *Journal of research in science teaching*, 27:937–949, 1990.
- [106] J. Oh and K. Lee. On the effectiveness of supervision in asymmetric non-contrastive learning. In *Proceedings of Machine Learning Research*, 2024.
- [107] S. Ontañón. An overview of distance and similarity functions for structured data. *Artificial Intelligence Review*, 53:5309–5351, 2020.
- [108] S. Ontañón and E. Plaza. Similarity measures over refinement graphs. *Machine learning*, 87:57–92, 2012.



- [109] H. Owhadi. Computational graph completion. *Research in the Mathematical Sciences*, 9(2):27, 2022.
- [110] C. H. Papadimitrios and K. Steiglitz. *Combinatorial optimization: algorithms and complexity*. Courier Corporation, 1998.
- [111] R. Parello, Y. Gourinat, E. Benard, and S. Defoort. Structural sizing of a hydrogen tank for a commercial aircraft. In *Journal of Physics: Conference Series*, volume 2716, page 012040. IOP Publishing, 2024.
- [112] A. Payandeh, K. Baghaei, P. Fayyazsanavi, S. Ramezani, Z. Chen, and S. Rahimi. Deep representation learning: Fundamentals, technologies, applications, and open challenges. *IEEE Access*, 11:137621–137659, 2023.
- [113] J. Pelamatti, L. Brevault, M. Balesdent, E.-G Talbi, and Y. Guerin. Bayesian optimization of variable-size design space problems. *Optimization and Engineering*, 22:387–447, 2021.
- [114] J. Pelamatti, L. Brevault, M. Balesdent, E.-G. Talbi, and Y. Guerin. Bayesian optimization of variable-size design space problems. *Optimization and Engineering*, 22:387–447, 2021.
- [115] J. Poole and J. Campbell. A novel algorithm for matching conceptual and related graphs. In *Conceptual Structures: Applications, Implementation and Theory: Third International Conference on Conceptual Structures, ICCS’95 Santa Cruz, CA, USA, August 14–18, 1995 Proceedings 3*, 1995.
- [116] M. J. D. Powell. *A direct search optimization method that models the objective and constraint functions by linear interpolation*, volume 275, pages 51–67. Springer, 1994.
- [117] M. Quillian. The teachable language comprehender: A simulation program and theory of language. *Communications of the ACM*, 12:459–476, 1969.
- [118] R. Rada, H. Mili, E. Bicknell, and M. Blettner. Development and application of a metric on semantic nets. *IEEE transactions on systems, man, and cybernetics*, 19:17–30, 1989.
- [119] D. Ramachandram, M. Lisicki, T. Shields, M. Amer, and G. Taylor. Bayesian optimization on graph-structured search spaces: Optimizing deep multimodal fusion architectures. *Neurocomputing*, 298:80–89, 2018.
- [120] M. Ramoni, P. Sebastiani, and P. Cohen. Bayesian clustering by dynamics. *Machine learning*, 47:91–121, 2002.
- [121] B. Recht, R. Roelofs, N. Srebro, M. Stern, and A.C. Wilson. The Marginal Value of Adaptive Gradient Methods in Machine Learning. In *Advances in Neural Information Processing Systems*, NIPS17. Curran Associates Inc., 2017.
- [122] A. Remadi, K. El Hage, Y. Hobeika, and F. Bugiotti. To prompt or not to prompt: Navigating the use of large language models for integrating and modeling heterogeneous data. *Data & Knowledge Engineering*, 152:102313, 2024.
- [123] O. Renkonen. Statisch-kologische untersuchungen ber die terrestrische kaferwelt der finnischen bruchmoore. *Annales Botanici Societatis Zoologic-Botanic Fennic Vanamo*, 6:1231, 1938.
- [124] P. Resnik. Semantic similarity in a taxonomy: An information-based measure and

- its application to problems of ambiguity in natural language. *Journal of artificial intelligence research*, 11:95–130, 1999.
- [125] P. Robert and Y. Escoufier. A unifying tool for linear multivariate statistical methods: the rv-coefficient. *Journal of the Royal Statistical Society Series C: Applied Statistics*, 25(3):257–265, 1976.
  - [126] A. Robles-Kelly and E. Hancock. Graph edit distance from spectral seriation. *IEEE transactions on pattern analysis and machine intelligence*, 27:365–378, 2005.
  - [127] A. Robles-Kelly and E. Hancock. String edit distance, random walks and graph matching. *International Journal of Pattern Recognition and Artificial Intelligence*, 18:315–327, 2004.
  - [128] S. Roussel, T. Polacsek, and A. Chan. Assembly line preliminary design optimization for an aircraft. In *CP 2023 (The 29th International Conference on Principles and Practice of Constraint Programming)*, 2023.
  - [129] W. Sager and P. Lockeman. Classification of ranking algorithms. *International Forum on Information and Documentation*, 1976.
  - [130] P. Saves. *High-dimensional multidisciplinary design optimization for aircraft eco-design/Optimisation multi-disciplinaire en grande dimension pour l’eco-conception avion en avant-projet*. PhD thesis, ISAE-SUPAERO, 2024.
  - [131] P. Saves, J. Bussemaker, R. Lafage, Thierry T. Lefebvre, Nathalie Bartoli, Youssef Diouane, and Joseph Morlier. System-of-systems modeling and optimization: An integrated framework for intermodal mobility. In *ODAS 2024: 24th joint ONERA-DLR Aerospace Symposium*, 2024.
  - [132] P. Saves, Y. Diouane, N. Bartoli, T. Lefebvre, and J. Morlier. A mixed-categorical correlation kernel for Gaussian process. *Neurocomputing*, 550:126472, 2023.
  - [133] P. Saves, Y. Diouane, N. Bartoli, T. Lefebvre, and J. Morlier. High-dimensional mixed-categorical gaussian processes with application to multidisciplinary design optimization for a green aircraft. *Structural and Multidisciplinary Optimization*, 67:81, 2024.
  - [134] P. Saves, Y. Diouane, N. Bartoli, T. Lefebvre, and J. Morlier. High-dimensional mixed-categorical gaussian processes with application to multidisciplinary design optimization for a green aircraft. *Structural and Multidisciplinary Optimization*, 67:81, 2024.
  - [135] P. Saves, R. Lafage, N. Bartoli, Y. Diouane, J. H. Bussemaker, T. Lefebvre, J. T. Hwang, J. Morlier, and J. R. R. A. Martins. SMT 2.0: A surrogate modeling toolbox with a focus on hierarchical and mixed variables Gaussian processes. *Advances in Engineering Software*, 188:1–15, 2024.
  - [136] P. Saves, E. Nguyen Van, N. Bartoli, Y. Diouane, T. Lefebvre, C. David, S. Defoort, and J. Morlier. Bayesian optimization for mixed variables using an adaptive dimension reduction process: applications to aircraft design. In *AIAA SciTech 2022 Forum*, 2022.
  - [137] P. Schmollgruber, C. Döll, J. Hermetz, R. Liaboeuf, M. Ridet, I. Cafarelli, O. Atinault, C. François, and B. Paluch. Multidisciplinary exploration of DRAGON: an ONERA hybrid electric distributed propulsion concept. In *AIAA SciTech 2019 Forum*, 2019.
  - [138] J. Serra and J. Arcos. An empirical evaluation of similarity measures for time series classification. *Knowledge-Based Systems*, 67:305–314, 2014.

- [139] F. Serratos. Redefining the graph edit distance. *SN Computer Science*, 2:438, 2021.
- [140] B. Shahriari, K. Swersky, Z. Wang, R. P. Adams, and N. de Freitas. Taking the Human Out of the Loop: A Review of Bayesian Optimization. *Proceedings of the IEEE*, 104:148–175, 2016.
- [141] James M Shihua, Paul Saves, Rhea P Liem, and Joseph Morlier. Bayesian optimization of a lightweight and accurate neural network for aerodynamic performance prediction. *arXiv preprint arXiv:2503.19479*, 2025.
- [142] W.L. Simmons. *A Framework for Decision Support in Systems Architecting*. PhD thesis, Massachusetts Institute of Technology, 2008. Available at <https://dspace.mit.edu/handle/1721.1/42912>.
- [143] G. Song, D. Fu, and D. Zhang. From knowledge graph development to serving industrial knowledge automation: a review. In *2022 Chinese Control Conference*, 2022.
- [144] T. Sorensen. A method of establishing groups of equal amplitude in plant sociology based on similarity of species content and its application to analyses of the vegetation on danish commons. *Biologiske skrifter*, 5:1–34, 1948.
- [145] B. Sow, R. Le Riche, J. Pelamatti, S. Zannane, and M. Keller. Learning functions defined over sets of vectors with kernel methods. In *UNCECOMP*, 2023.
- [146] H. Steck, C. Ekanadham, and N. Kallus. Is cosine-similarity of embeddings really about similarity? In *Companion Proceedings of the ACM on Web Conference 2024*, 2024.
- [147] D. Streitferdt, M. Riebisch, and K. Philippow. Details of formalized relations in feature models using OCL. In *10th IEEE International Conference and Workshop on the Engineering of Computer-Based Systems, 2003. Proceedings.*, pages 297–304. IEEE, 2003.
- [148] G. Székely and M. Rizzo. Brownian distance covariance. *The Annals of Applied Statistics*, 3(4):1236–1265, 2009.
- [149] E-G. Talbi. Metaheuristics for (variable-size) mixed optimization problems: A unified taxonomy and survey. *ArXiv preprint*, 2024.
- [150] T. Tanimoto. Elementary mathematical theory of classification and prediction. *International Business Machines Corp.*, 1958.
- [151] A. Tversky and I. Gati. Studies of similarity. *Cognition and categorization*, 1:79–98, 1979.
- [152] J. Valls-Vargas, J. Zhu, and S. Ontanon. Error analysis in an automated narrative information extraction pipeline. *IEEE Transactions on Computational Intelligence and AI in Games*, 9:342–353, 2016.
- [153] J. von Kügelgen, M. Besserve, L. Wendong, L. Gresele, A. Kekić, E. Bareinboim, D. Blei, and B. Schölkopf. Nonparametric identifiability of causal representations from unknown interventions. *Advances in Neural Information Processing Systems*, 37:1–36, 2024.
- [154] W. Wallis, P. Shoubridge, M. Kraetz, and D. Ray. Graph distances using graph union. *Pattern Recognition Letters*, 22:701–704, 2001.
- [155] Y. Wang and N. Ishii. A method of similarity metrics for structured representations.

- Expert Systems with Applications*, 12:89–100, 1997.
- [156] W. Winkler. Matching and record linkage. *Wiley interdisciplinary reviews: Computational statistics*, 6:313–325, 2014.
  - [157] P. Winter and S. MacGregor. Path-distance heuristics for the steiner problem in undirected networks. *Algorithmica*, 7:309–327, 1992.
  - [158] H. Wu, H. Yang, X. Li, and H. Ren. Semi-supervised autoencoder: A joint approach of representation and classification. In *Proceedings of the 2015 International Conference on Computational Intelligence and Communication Networks (CICN)*, 2016.
  - [159] M. Zaefferer and D. Horn. A first analysis of kernels for Kriging-based optimization in hierarchical search spaces. *ArXiv preprint*, 2018.